

BIOCHEMICAL ANALYSIS OF APOPTOSOME FORMATION

APPROVED BY SUPERVISORY COMMITTEE

Dr. John Abrams

Dr. Zhijian James Chen

Dr. Michael Rosen

Dr. Xiaodong Wang

DEDICATION

I would like to thank the members of my thesis committee for their encouragement throughout my graduate study. They shared their enthusiasm toward science with me and inspired me to pursue the fundamental scientific questions by all means. I can not say enough thank to my mentor, Dr. Xiaodong Wang. He is the best mentor you could wish for. He has been very patient with his students and he cares about them. You can feel he cares so much for students' development as scientists. He offers his wisdom, expertise as a biochemist, and perspectives. His passion toward solving the scientific questions is almost infectious. He trains us to raise questions, develop hypothesis, and execute experiments, independently. At the same time when he allows us to work independently, he is always there for us whenever he is needed. I feel privileged to learn from him.

I also want to thank our lab people for their support. As a foreign student studying abroad, it has been tough for me to live apart from my family. Our lab people provided me a place like home so that I can feel safe and confident in the lab. Xuejun, Fenghe, and Lai helped me with their expertises. Xuejun taught me how to plan the daily experiments and deal with the frustration in the lab. He always sees the positive site and cheers me up with

his high spirit. I learned a lot from him. Lai and Asli became my best friends in the lab. I feel so lucky to work with them in the same lab.

And last, I want thank my family for their strong support for my whole life. My mother has been my strongest supporter and believes in me more than I do. My brother is the reason I could study so far away from my parents without worrying about my ‘getting old’ parents. He is the bridge between me and my parents who cares for my family the most. My aunt Hyesook and her husband Sooyoung have been my biggest fans who pray for me all the time. They inspire me with their deep love and generosity. I can not thank enough to them for what they have done to me.

BIOCHEMICAL ANALYSIS OF APOPTOSOME FORMATION

By

Hyun-Eui Kim

DISSERTATION

Presented to the Faculty of the Graduate School of Biomedical Sciences

The University of Texas Southwestern Medical Center at Dallas

In Partial Fulfillment of the Requirements

For the Degree of

DOCTOR OF PHILOSOPHY

The University of Texas Southwestern Medical Center at Dallas

Dallas, Texas

August, 2006

BIOCHEMICAL ANALYSIS OF APOPTOSOME FORMATION

Hyun-Eui Kim

The University of Texas Southwestern Medical Center at Dallas, 2006

Supervising Professor: Xiaodong Wang, Ph.D.

Apoptosis is an active cell death program executed by proteases named caspases. One of the major caspase-activating pathways is initiated by mitochondria. Upon various apoptotic stimuli, the mitochondria releases cytochrome *c* into the cytosol where it binds to apoptotic protease activating factor 1 (Apaf-1). Then, the cytochrome *c*-bound Apaf-1 forms a heptameric complex named apoptosome. Apoptosome provides a platform to activate downstream caspases. The initiator caspase, procaspase-9 is recruited to apoptosome and gets activated to cleave downstream effector caspases. The series of this activation cascade is tightly regulated at each step. However, the role of cytochrome *c* and nucleotides during apoptosome formation is not clear.

Also, how the apoptosome activity is stimulated by the positive regulator PHAP proteins is yet to be determined. Thus, my thesis work includes studies regarding these questions using biochemical analysis. I reconstituted apoptosome pathway using recombinant proteins *in vitro*. As a result, I discovered several biochemical steps during apoptosome formation that were previously unknown. And I identified a new mediator that positively regulates apoptosome formation. The new findings are, 1) Recombinant Apaf-1 obtained from insect cell expression system was already associated with dATP. 2) The Apaf-1-bound dATP got hydrolyzed upon cytochrome *c* binding. 3) The hydrolyzed nucleotide on Apaf-1 needed to be exchanged with dATP/ATP to form an active apoptosome. 4) CAS is a mediator of PHAP proteins. PHAPI and CAS enhanced the nucleotide exchange on Apaf-1 to stimulate apoptosome formation.

TABLE OF CONTENTS

PRIOR PUBLICATIONS.....	ix
LIST OF FIGURES.....	x
LIST OF ABBREVIATIONS.....	xii
CHAPTER ONE Introduction.....	1
Apoptosis and caspases.....	1
Caspase activation.....	3
Structure of Apaf-1 and apoptosome.....	7
Heat shock proteins and mitochondria-mediated apoptosis.....	9
Regulation of apoptosome function.....	11
CHAPTER TWO Abstract.....	22
Introduction.....	23
PETCM stimulates apoptosome formation and caspase-3 activation.....	24
ProT inhibits caspase-3 activation and PETCM antagonizes the inhibitory activity.....	27
ProT and PHAP distinctively regulate apoptosome formation and activity.....	28
Elimination of ProT in vivo sensitizes HeLa cells to an apoptotic stimulus and bypasses PETCM action.....	29
ProT and PHAP as apoptotic regulators.....	30
Experimental Procedures.....	32
Figures.....	40
CHAPTER THREE Abstract.....	46
Introduction.....	46
Reconstitution of caspase-3 activation using purified protein components.....	50

Preincubation of Apaf-1 and cytochrome <i>c</i> without dATP inactivates Apaf-1.....	51
Apaf-1 contains a dATP cofactor.....	53
Cytochrome <i>c</i> induces dATP hydrolysis.....	54
Nucleotide exchange on Apaf-1 during apoptosome formation.....	55
Discussion.....	56
Experimental Procedures.....	59
Figures.....	64
CHAPTER FOUR Abstract.....	70
Introduction.....	71
<i>In vitro</i> reconstitution of PHAPI pathway.....	74
Identification of CAS as a mediator of PHAPI.....	76
Total <i>in vitro</i> reconstitution with recombinant proteins.....	78
PHAPI and CAS help dATP exchange.....	80
<i>In vivo</i> knock down of CAS.....	82
Experimental Procedures.....	88
Figures.....	96
SUMMARY.....	102
REFERENCES.....	106
VITAE.....	118

Prior publications

1. Jiang, X., Kim, H-E., Shu, H., Zhao, Y., Zhang, H., Kofron, J., Donnelly, J., Burns, D., Ng, S-c., Rosenberg, S., Wang, X. (2003). Distinctive roles of PHAP proteins and prothymosin- α in a death regulatory pathway. *Science* 299 (5604); 223-226.
2. Liu, Q., Rand, T.A., Kalidas, S., Du, F., Kim, H-E., Smith, D.P., Wang, X. (2003). R2D2, a bridge between the initiation and effector steps of the *Drosophila* RNAi pathway. *Science* 301 (5641); 1921-1925.
3. Kim, H-E., Du, F., Fang, M., Wang, X. (2005). Formation of apoptosome is initiated by cytochrome *c*-induced dATP hydrolysis and subsequent nucleotide exchange on Apaf-1. *Proc Natl Acad Sci U S A* 102 (49); 17545-17550.

LIST OF FIGURES

CHAPTER ONE

FIGURE 1-1.....	14
FIGURE 1-2.....	15
FIGURE 1-3.....	16
FIGURE 1-4.....	17
FIGURE 1-5.....	18
FIGURE 1-6.....	19
FIGURE 1-7.....	20
FIGURE 1-8.....	21

CHAPTER TWO

FIGURE 2-1.....	40
FIGURE 2-2.....	41
FIGURE 2-3.....	42
FIGURE 2-4.....	43
FIGURE 2-5.....	44
FIGURE 2-S1.....	45

CHAPTER THREE

FIGURE 3-1.....	64
FIGURE 3-2.....	66
FIGURE 3-3.....	67
FIGURE 3-4.....	68
FIGURE 3-5.....	69

CHAPTER FOUR

FIGURE 4-1.....96

FIGURE 4-2.....97

FIGURE 4-3.....98

FIGURE 4-4.....99

FIGURE 4-5.....100

FIGURE 4-6.....101

LIST OF ABBREVIATIONS

Apaf-1: apoptotic protease activating factor 1

CARD: caspase recruitment domain

CAS: cellular apoptosis susceptibility protein

Cyt.c: cytochrome *c*

DED : death effector domain

NOD: nucleotide binding and oligomerization domain

PETCM: α -(trichloromethyl)-4-pyridineethano

PHAP: putative HLA-DR-associated proteins

ProT: prothymosin- α

Chapter 1 : Introduction

Apoptosis and Caspases

Apoptosis plays an important role in development, tissue homeostasis and pathology. During development, specific cell populations need to be cleared up for patterning organs and tissues (Meier et al., 2000). Also apoptosis is a major type of cell death for cellular homeostasis. Therefore, apoptosis and cell survival signaling is meticulously balanced throughout organisms' life. When this balance is disturbed, it can cause numerous pathological conditions such as defects in development, neurodegenerative diseases, cancers or autoimmune disease (Thompson, 1995). Apoptosis is a programmed cell death featuring characteristic morphological changes during cell death. These features include cell membrane blebbing, cell shrinkage, DNA fragmentation, nuclear condensation and fragmentation, and breaking down into apoptotic bodies, which are engulfed by neighboring cells (Wyllie, 1980; Savill and Fadok, 2000).

The characteristic morphological changes in cells undergoing apoptosis are the result of caspase activation. Caspases are a family of cysteine proteases that cleave their substrates after aspartate residues. To date, about 14 caspases are identified in a mammalian system (Figure 1; adopted from Shi, 2002).

(Stennicke and Salvesen, 2000). Caspases are produced as zymogens that are inactive (procaspases). Caspases consist of a prodomain followed by large (p20) and small (p10) subunits. Except for caspase-9, proteolytic cleavage is required for activation of procaspase zymogens. Caspases are classified into three groups such as inflammatory caspases, apoptotic initiator caspases and apoptotic effector caspases (Degterev et al., 2003). Caspase-1, -4, -5, -11, -12, -13 and -14 are inflammatory caspases, nonetheless, caspase-14 is unique as its activation is associated with epithelial cell differentiation. Caspase-2, -9, -8, and -10 are apoptotic initiator caspases. The initiator caspases contain the long prodomains with death effector domain (DED) for caspase-8 and -10 or caspase recruitment domain (CARD) for caspase-2 and -9. Initiator caspases get activated through the protein-protein interaction using DED or CARD domains. Apoptotic effector caspases include caspase-3, -6, and -7, which have shorter prodomains. They are also called as executioner caspases because they get activated by upstream initiator caspases and execute the downstream apoptotic events by cleaving their substrates. Their targets can be mediators and regulators of apoptosis such as Bid and ICAD, the structural proteins, cellular DNA repair proteins such as DNA-PK and ATM proteins, and cell cycle-related proteins (Degterev, 2003).

Caspase activation

Apoptotic stimuli trigger activation of initiator caspases. The initiator caspases are activated by two distinct pathways, the extrinsic and intrinsic pathways depending on the type of apoptotic stimuli (Chen and Wang, 2002). The extrinsic pathway is initiated by binding of extracellular ligands (such as TNF, FasL, or TRAIL) to their cognate cell surface death receptors (TNFR, Fas, DR4 or DR5). Binding of ligands to their cognate receptors promotes the recruitment of adaptor proteins to the membrane. Using protein-protein interaction between death domain on the receptor and adaptor proteins, they form a death-inducing signaling complex (DISC). The DISC recruits procaspase-8 or -10 (mostly in lymphoid cells), and activates it. Figure 2 (adopted from Schafer and Kornbluth, 2006) shows one of the death receptor-mediated caspase activation (Fas-mediated apoptosis). The activated caspase-8 can directly activate the downstream effector caspases or cleave Bid protein to trigger mitochondria-induced apoptosis (in Fas and TRAIL-mediated apoptosis). The cleaved Bid (tBid) translocates to the mitochondria and disrupts mitochondrial integrity to promote cytochrome *c* release (Figure 2). Even though the extrinsic pathways triggered by different ligands share the common principle to activate upstream initiator caspases, the components of complexes and their downstream targets vary depending on the responsive death receptors. For example, TNF can activate various cellular responses

through activation of NF- κ B, JNK and apoptosis (Baud and Karin, 2001). It can form two different complexes such as complex I and II. In brief, complex I thought be composed with TNFR1, TRADD, TRAF2, and RIP and recruits IKK complex to activate NF- κ B pathway or complex I also can activate JNK pathway. Complex II is thought to be dissociated from the membrane and released to the cytosol to recruit caspase-8 or 10 and activate it. Yet, the composition and existence of complex I and II are still controversial. Unlike Fas and TRAIL, TNF induces a pro-survival pathway through NF- κ B activation. Only when the NF- κ B activation is blocked, TNF can induce cell death (Wang et al., 1996). FasL and TRAIL induced signaling pathways are similar. FasL and TRAIL activate caspase-8 to induce apoptosis and the same time they can also induce the intrinsic pathway by cleaving the Bid into truncated Bid (tBid).

The intrinsic pathway is initiated from the mitochondria in response to apoptotic stresses such as DNA damage and growth factor withdrawal or signaling from death receptor-mediated pathway such as tBid (Figure 2). The mitochondria initiate apoptosis signaling by releasing cytochrome *c* into the cytosol. Apaf-1 is a binding partner of cytochrome *c* in the cytosol. The cytochrome *c* -bound Apaf-1 then, assembles a heptameric complex named apoptosome in the presence of dATP/ATP (Liu et al., 1996; Zou et al., 1997).

Apoptosome serves as a platform to recruit procaspase-9 and activate downstream caspases (Figure 2). Caspase activation through the apoptosome pathway is conserved in worm and fly, even though the structure and regulation mechanism are slightly different in each organism (Kornbluth and White, 2005). In *C. elegans*, caspase CED-3 is activated by the worm apoptosome assembled with a tetramer of CED-4 molecules and regulated by the anti-apoptotic bcl-2 protein CED-9 and the pro-apoptotic BH3-only protein EGL-1 (Figure 3, adopted from Adrain et al., 2006). In *Drosophila*, CED-4 homolog Dark, also known as Hac-1 or dApaf-1 assembles an octamer complex as an apoptosome and activates caspase Dronc. Dronc is inhibited by DIAP in a similar mechanism to that of mammalian IAPs. And in response to apoptotic stimuli, DIAP is neutralized by Reaper, Hid and Grim proteins.

The mammalian apoptosome contains a heptamer of Apaf-1. Apoptosome formation is regulated by Bcl-2 family of proteins upstream of the mitochondria. Anti-apoptotic Bcl-2 family of proteins such as Bcl-2, Bcl-xL and Mcl-1 protect the integrity of the mitochondrial membrane. On the contrary, pro-apoptotic Bcl-2 family members, also known as BH3-only proteins such as Bid, Bad, Bin, Noxa and Puma disrupt the mitochondrial integrity and initiate the mitochondria-mediated intrinsic apoptosis pathway (reviewed in Willis and Adams, 2005). The BH3-only proteins such as Bim,

Bik and Bad neutralize anti-apoptotic Bcl-2 family of proteins by binding to them on the mitochondria. Ultimately, the pro-apoptotic Bcl-2 family member of proteins such as Bax and Bak oligomerize on the mitochondria and disrupt the membrane integrity. Then, cytochrome *c* is released into the cytosol and induces apoptosis.

The mitochondria not only release cytochrome *c* to the cytosol to promote apoptosome formation, but also release other pro-apoptotic proteins such as AIF (Susin et al., 1999), EndoG (Li et al., 2001; Parrish et al., 2001), Smac/Diablo (Du et al., 2000; Werhagen et al., 2000), and HtrA2/Omi (Vaux and Silke, 2003). AIF and Endo G are involved in the DNA fragmentation at a relatively later stage of apoptosis. Smac and Omi are involved in neutralizing IAPs so that caspase-9 and caspase-3 can be activated.

The IAP (inhibitor of apoptosis) family of proteins includes cIAP1, cIAP2, XIAP, NAIP, BRUCE, survivin and ML-IAP/livin. IAP was originally identified from baculovirus infected insect cells based on its ability to inhibit caspases. All members of IAP protein family contain the functional unit named BIR (baculoviral IAP repeat) domains and C-terminal RING (really interesting new gene) domain in the XIAP, cIAP1, cIAP2, and livin (Shi, 2002). The BIR domains have a zinc-finger-like structure that can bind to the caspases. BIR1 and BIR2 domains of IAPs inhibit caspase-3 and -7, while the BIR3 domain

inhibits caspase-9. XIAP, cIAP1 and cIAP2 can bind to procaspase-9 and prevent it from activation (Deveraux et al., 1998). Thus, IAPs can inhibit the apoptosome-mediated caspase activation effectively, even after cytochrome *c* is released from the mitochondria. The tetrapeptide motif in caspase-9 (ATPF in human and AVPY in mouse), interacts with the BIR3 domain of XIAP. Smac also contains an AVPI motif at its N-terminus after the mitochondrial targeting signal peptide. When Smac protein is targeted to the mitochondria, the signal peptide is cleaved-off. Therefore, the Smac released from mitochondria contains the AVPI motif at the N-terminus and neutralizes XIAP to release caspase-9 from XIAP inhibition (Wu et al., 2000). Omi binds to BIR2 and BIR3 of XIAP using its tetrapeptide AVPS motif (Van Loo et al., 2002). The overall mechanism of mitochondrial-released proteins in apoptosis described above is summarized in Figure 4 (adopted from Saelens et al., 2004).

Structure of Apaf-1 and apoptosome

The Apaf-1 protein consists of a C-terminal caspase recruitment domain (CARD) followed by a nucleotide binding and oligomerization domain (NOD) also called ced-4 domain (Figure 5; adopted from Acehan et al., 2002), and a linker region flanked by WD-40 repeats. The Apaf-1 has several alternatively spliced isoforms that differ in the number of WD-40 repeats (12

or 13), or the presence of additional sequences between the CARD domain and the ced-4 domain (Fu et al., 2001; Hahn et al., 1999; Benedict et al., 2000).

The cytochrome *c* binds to the WD-40 repeats and Apaf-1 forms a heptameric apoptosome in the presence of dATP/ATP. Then, the procaspase-9 is recruited to the apoptosome by protein-protein interaction between the CARD domains in both procaspase-9 and Apaf-1 (Li et al., 1997). The definition of the 3-dimensional structure of the apoptosome at 27 Å resolution using cryo-electronmicroscopy indicates that the apoptosome is a wheel like structure with a central hub, which is connected to 7 spokes (Acehan et al., 2002). This model predicts the central hub domain is formed by the CARD domains of seven Apaf-1 molecules and the N-terminal portions of ced-4 domains. In addition, the ced-4 domains form spokes that projected outward from the central hub. And the WD-40 repeats domains are connected to the spokes forming Y shape domain (Figure 5 and Figure 6; adopted from Acehan et al., 2002). The Y-domain has 2 lobes, one small and the other large. These two lobes fit to 6- and 7- WD-40 repeats folding a β -propeller structure. The cytochrome *c* binds to the Y-domain between the two lobes.

In the absence of cytochrome *c*, monomer Apaf-1 stays as in an autoinhibitory conformation. According to Acehan et al., the CARD domain is bound to the Y shape β -propellers. Binding of cytochrome *c* in the Y shape

lobes (WD-40 repeats) would induce the conformational change in Apaf-1 by replacing the CARD domain. This would promote apoptosome assembly and procaspases recruitment using CARD-CARD interaction. In the presence of noncleavable mutant of procaspase-9, apoptosome forms the similar wheel-like structure with an additional dome-like structure on top of the central hub region. The dome-like structure contacts the hub region where the CARD domain of Apaf-1 is predicted to be (Figure 7; adopted from Acehan et al., 2002).

The recent result from the crystal structure of WD-40-deleted Apaf-1 provided more insights to the function of nucleotides in apoptosome (Riedl et al., 2005). The WD-40-deleted Apaf-1 obtained from bacteria is associated with ADP buried deep inside Apaf-1's domains locking the Apaf-1 as an inactive state. Since WD-40-deletion may mimic the state of cytochrome *c*-bound Apaf-1, cytochrome *c* may promote hydrolysis of dATP/ATP to promote apoptosome formation. The detailed biochemical function of cytochrome *c* and nucleotides is discussed in chapter 3.

Heat shock proteins and mitochondria-mediated apoptosis

Induction of protein expression of heat shock proteins (Hsps) in response to cellular stress can prevent apoptosis induced by both intrinsic and

extrinsic pathways (Beere, 2005). Hsp90, Hsp70, and Hsp27 are member of Hsp proteins that are well known to have antiapoptotic functions. Hsp70 and Hsp90 proteins consist of highly conserved N-terminal ATPase domains and C-terminal substrate binding sites. The C-terminal four amino acids, EEVD are essential for their function (Li et al., 1992). Hsp70 protein is a master protein in the cellular stress response system. Hsp70 has been known to bind to Apaf-1 to inhibit apoptosome formation and/or to inhibit procaspase-9 recruitment to apoptosome (Beere et al., 2000; Saleh et al., 2000). However, whether Hsp70 inhibits apoptosome formation via its interaction with Apaf-1 is not clear. With a recent report from Steel et al., it seems rather unlikely (Steel et al., 2004). Nonetheless, both Hsp70 and Hsp90 seem to be able to inhibit apoptosome-mediated apoptosis by controlling various steps during apoptosis.

Hsp70 can prevent apoptosis both upstream and downstream of the mitochondria (Figure 5). Both Hsp70 and Hsp27 can regulate Bid-mediated apoptosis by suppressing Bid translocation to the mitochondria (Gabai et al., 2002; Paul et al., 2002). Also with a co-chaperone Hsp40, Hsp70 prevents Bax translocation in response to TNF (Gotoh et al., 2004). Through Bid and Bax suppression, Hsp70 can protect mitochondrial integrity. On the other hand, Hsp70 can bind to AIF (Susin et al., 1999), which is released from the mitochondria. Hsp70 binds to AIF and inhibit its translocation into the nucleus

(Ravagnan et al., 2001; Gurbuxani et al., 2003). Interestingly Hsp70 is also involved in apoptosome-independent cell death in Apaf-1^{-/-} MEF cells (Ravagnan et al., 2001).

Hsp90 and Hsp27 also have been shown to inhibit apoptosome formation. Hsp90 binds to Apaf-1 to inhibit apoptosome formation (Pandey et al., 2000). Hsp27 may also prevent apoptosome formation by sequestering cytochrome *c* in the cytosol through its interaction with cytochrome *c* (Bruey et al., 2000). Hsp proteins can also affect several pro-survival signaling pathways mediated by Akt, JNK and NF- κ B. Hsp proteins regulate these signaling pathways mostly by modulating the stability of the proteins involved (Figure 8; adopted from Beere, 2005).

Regulation of apoptosome function

Apoptosome formation and its function can be regulated at various steps during apoptosis. As described above, regulation on mitochondrial level by Bcl-2 family of proteins can promote or inhibit apoptosome formation by controlling cytochrome *c* release from the mitochondria. Even after the apoptosome is formed its function can be blocked by IAPs, which protect caspases from being activated. Mitochondria-released proteins such as Smac and Omi can relieve this inhibition of IAPs by neutralizing them.

The biochemical steps leading to apoptosome formation is one of the well studied apoptotic pathways. However, the detailed function of cytochrome *c* and dATP/ATP on apoptosome formation remained to be determined. Is nucleotide hydrolysis required during apoptosome formation? Whether Apaf-1 hydrolyzes nucleotide during apoptosis is confusing, since the results are controversial depending on which nucleotide analog is used for the experiments (Zou et al., 1999; Jiang and Wang, 2000). Why do we need 1 mM of dATP to promote apoptosome formation using the cell lysates while the cellular level of dATP is around 10 μ M? The K_d for dATP binding is around 1.7 μ M (Jiang and Wang, 2000), yet require a lot more than that to induce apoptosome formation. We could speculate that there may be inhibitory molecules for apoptosome formation that need to be removed possibly by high concentration of dATP or there may be a specific nucleotide loading factor for Apaf-1.

In my thesis I want to discuss the questions above. Dr. Jiang, a previous member of our lab, discovered that the small molecule PETCM induces apoptosome-mediated caspase activation by removing the inhibitor of apoptosome formation. He identified a novel apoptosome regulatory pathway that consisted of positive and negative regulators (Chapter 2). In Chapter 2, I was involved in verifying the cellular function of both positive (PHAP

proteins) and negative (prothymosin- α) regulators using cancer cell lines. I used RNAi technique to knock down the regulators to test whether cell death phenotype is changed. I failed to knock down all of the PHAP proteins that are highly homologous and redundant, however I was able to knock down the expression of prothymosin- α . Thus I present the results of my *in vivo* study following the identification of this pathway that had been carried out by Dr. Jiang. In Chapter 3, I want to discuss the detailed biochemical steps during apoptosome formation and describe my observation on the function of dATP/ATP hydrolysis and exchange in addition to newly discovered property of cytochrome *c*-bound Apaf-1. Finally, in Chapter 4, I present the identification of a mediator of the apoptosome regulatory pathway described in Chapter 2. I identified CAS as a mediator of PHAP proteins and studied the mechanism of how PHAP proteins and CAS stimulate apoptosome activity. I developed total *in vitro* reconstitution assay to analyze the biochemistry involved in this pathway.

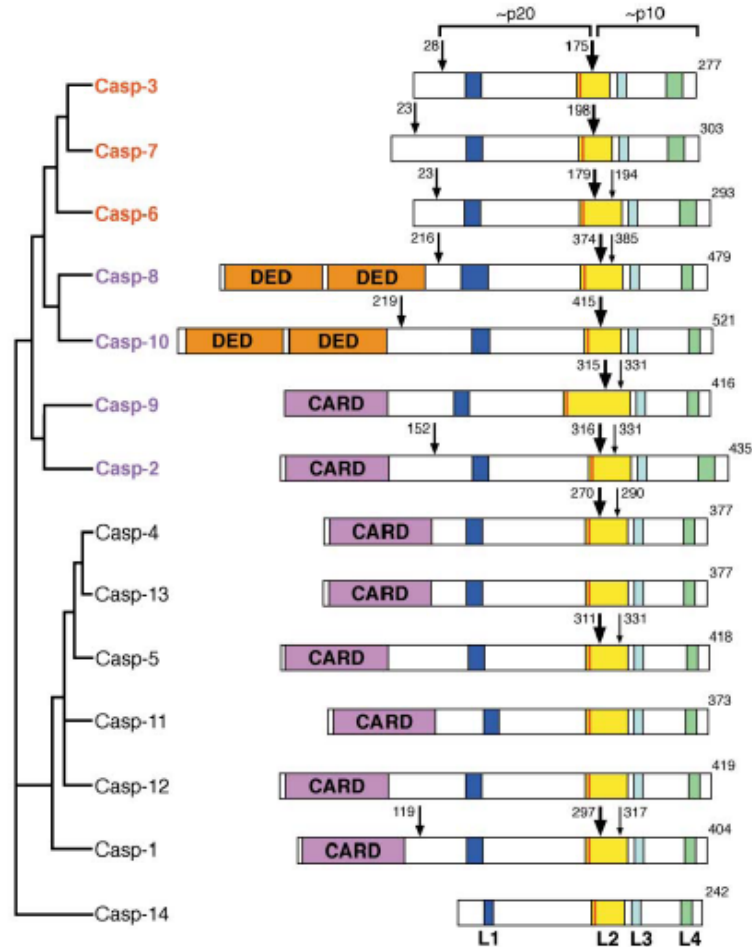


Figure 1-1. Schematic Diagram of the Mammalian Caspases

Except caspase-11 (mouse), -12 (mouse), and -13 (bovine), all listed caspases are of human origin. Their phylogenetic relationship (left) appears to correlate with their function in apoptosis or inflammation. The initiator and effector caspases are labeled in purple and red, respectively. The position of the first activation cleavage (between the large and small subunits) is highlighted with a large arrow while additional sites of cleavage are represented by medium and small arrows. In contrast to other protease zymogens, removal of the prodomain of a caspase is unnecessary for its catalytic activity. The four surface loops (L1-L4) that shape the catalytic groove are indicated. The catalytic residue Cys is shown as a red line at the beginning of loop L2. This diagram is scaled according to the lengths of caspases and the location of functional segments. (Adopted from Shi, 2002)

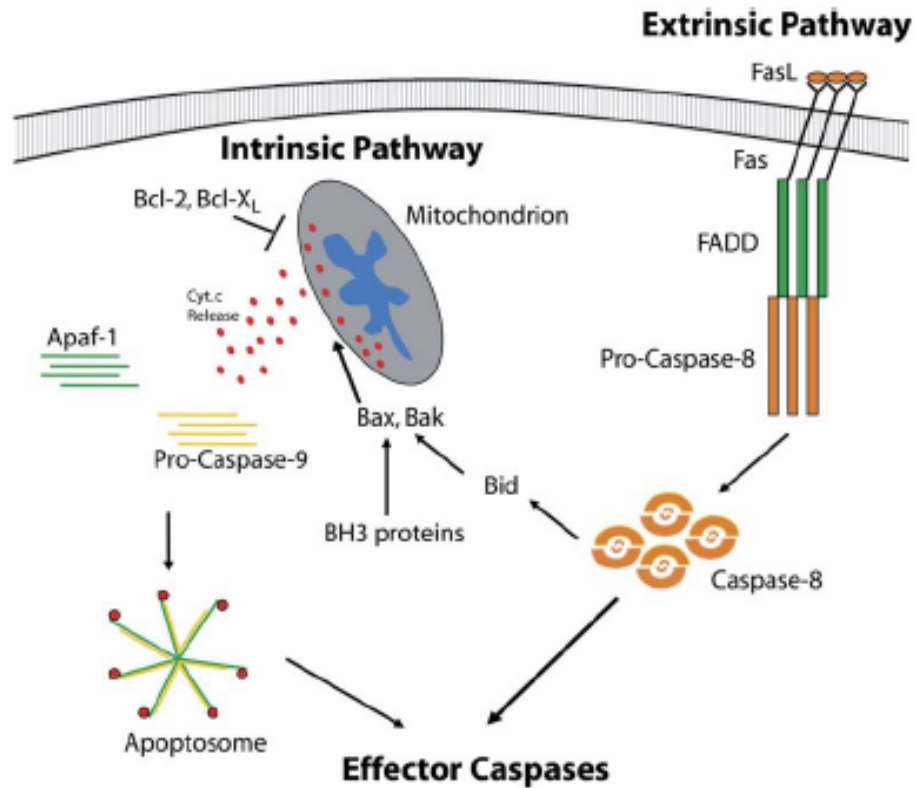


Figure 1-2. Caspase Activation via the Intrinsic and Extrinsic Pathways of Apoptosis
The activation of caspases during apoptosis proceeds through two distinct mechanisms. Activation of caspases through the extrinsic pathway involves the binding of extracellular ligands (e.g., FasL) to their cognate receptors (e.g., Fas) and the recruitment of intracellular adaptor proteins (e.g., FADD) to activate caspase- 8 and subsequent downstream effector caspases. The intrinsic pathway involves the release of cytochrome *c* from the mitochondria into the cytosol. This leads to the formation of the apoptosome, the activation of caspase- 9, and the cleavage of effector caspases. (Adopted from Schafer and Kornbluth, 2006)

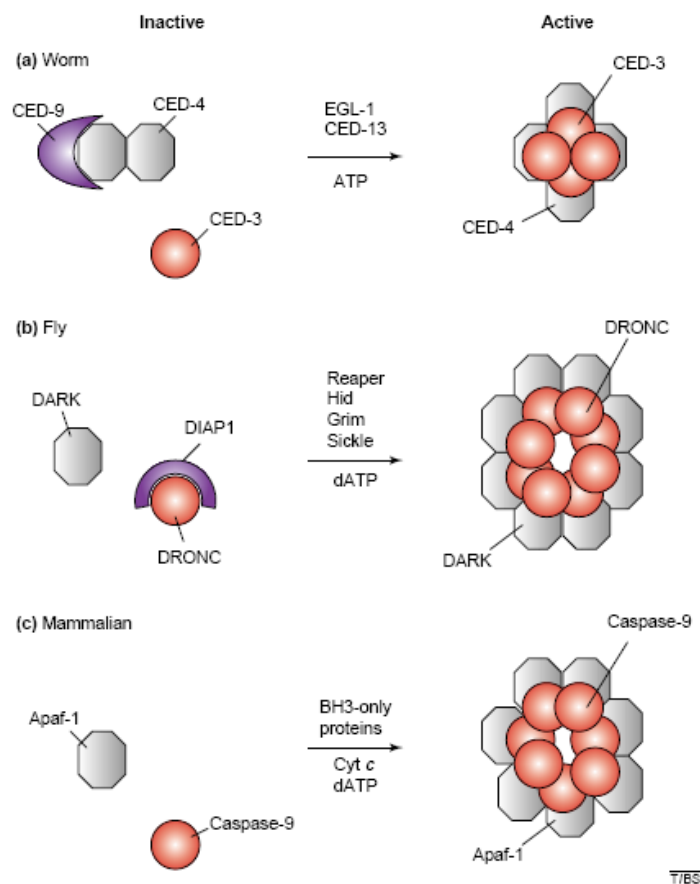


Figure 1-3. Assembly of worm, fly and human apoptosomes

(a) In the nematode worm, CED-4 (grey octagon) and CED-3 (red circle) can be induced to form apoptosomes through displacement of the cell-death-inhibitory protein, CED-9 (purple), from CED-4 dimers. CED-9 can be displaced by either of the BH3-only proteins EGL-1 or CED-13, and this permits the further dimerization of CED-4 dimers to form tetramers that can activate the CED-3 caspase. (b) In the fly, the CED-4-related protein, DARK (grey octagon), can oligomerize into an octameric structure that contains the CED-3-related protease DRONC (red circle). Fly apoptosomes are thought to be prevented from assembling through inhibition of DRONC by DIAP1. DIAP1 can be neutralized by the small proteins Reaper, Hid, Grim or Sickie (which are induced in response to specific stimuli) and this permits assembly of the octameric fly apoptosome. (c) In mammals, the CED-4-related protein Apaf-1 can be induced to oligomerize into heptameric apoptosomes that contain caspase-9. This is controlled by a family of proteins (the BH3-only members of the Bcl-2 family) that become activated in response to death triggers and liberate Cyt c from the mitochondrial intermembrane space. Cyt c acts as a co-factor for apoptosome assembly and, in association with dATP, triggers oligomerization of Apaf-1 and its association with caspase-9. (Adopted from Adrain et al., 2006)

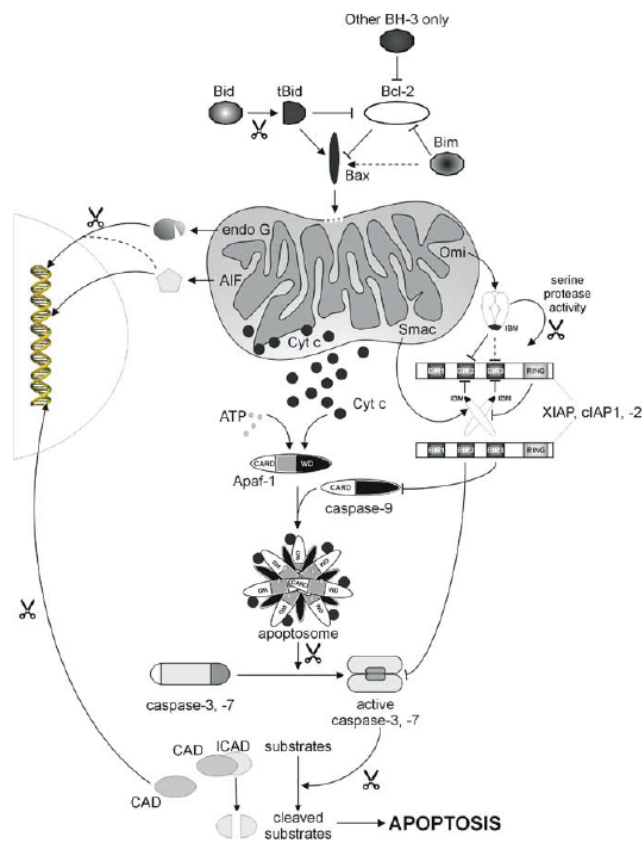


Figure 1-4. Multiple inner mitochondrial membrane proteins are released when the intrinsic apoptotic pathway is activated. Outer mitochondrial membrane integrity is mainly controlled by the Bcl-2 family proteins. BH-3-only proteins become active by different stress conditions. Bid for example is cleaved by a number of proteases including caspase-8, granzyme B and cathepsin B into tBid, which counteracts antiapoptotic Bcl-2 proteins and may directly activate Bax. Other BH-3-only proteins indirectly activate Bax by blocking antiapoptotic Bcl-2. Cytosolic cytochrome *c* (cyt *c*) will trigger apoptosome formation ensuing in a caspase cascade. Multiple cellular substrates are targeted by caspases, including ICAD that becomes inactivated by cleavage, thereby liberating CAD, which will translocate to the nucleus and start oligonucleosomal DNA fragmentation. IAPs prevent caspase-9 dimerization and block active caspase-3 and -7. Smac/DIABLO (Smac) and HtrA2/OMI (Omi) neutralize IAP inhibition by binding to the BIR2 and BIR3 domains. Dimeric Smac/DIABLO tethers BIR1 and BIR2, whereas HtrA2/ OMI preferentially binds BIR2 of XIAP. In addition, Omi can cleave IAPs through its serine protease activity. Smac is subject to proteasome-mediated degradation, as it is targeted by the ubiquitin–protein ligase activity residing in the C-terminal RING domain of XIAP and cIAP1 and cIAP2. Smac and Omi may also start a caspase-independent cell death pathway (not depicted). AIF and endonuclease G (endo G) translocate from the mitochondria to the nucleus, where they degrade nuclear DNA in a caspase independent way. (Adopted from Saelens et al., 2004)

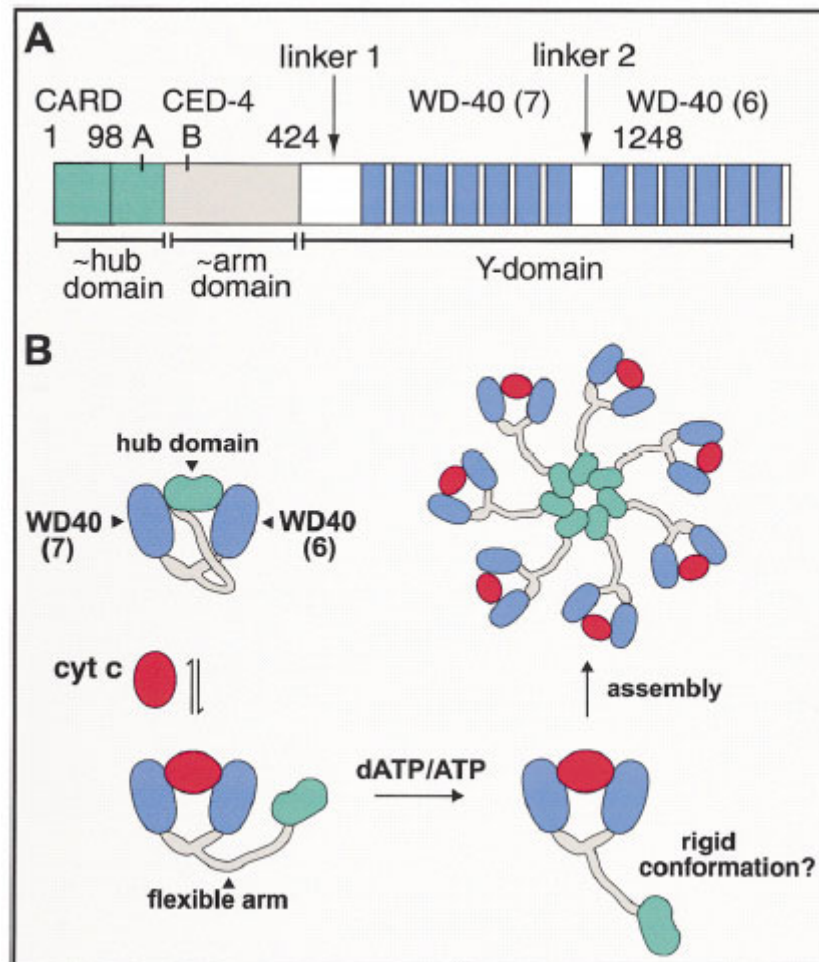


Figure 1-5. The Role of Apaf-1 Sequence Motifs in the Assembly of an Apoptosome
 (A) The relative positions of the CARD, CED4 homology motif, WD40 repeats, and linker regions are shown on a linear map of Apaf-1. The approximate positions of the hub, the arm, and the Y domains are indicated and color-coded. The positions of the Walker A and B nucleotide binding motifs are shown. Thus, the nucleotide binding pocket may be located in close proximity to the hub, where it may regulate assembly. (B) Apaf-1 normally adopts an autoinhibited conformation in healthy cells (top left). In actuality, only one globular region of the hub domain may interact directly with the β -propellers. Cytochrome c then displaces the hub domain (left side), which allows Apaf-1 to bind dATP/ATP (bottom). Upon nucleotide binding, a second conformational change may promote assembly (right side). For clarity, the length of the arm has been extended in this diagram. (Adopted from Acehan et al., 2002)

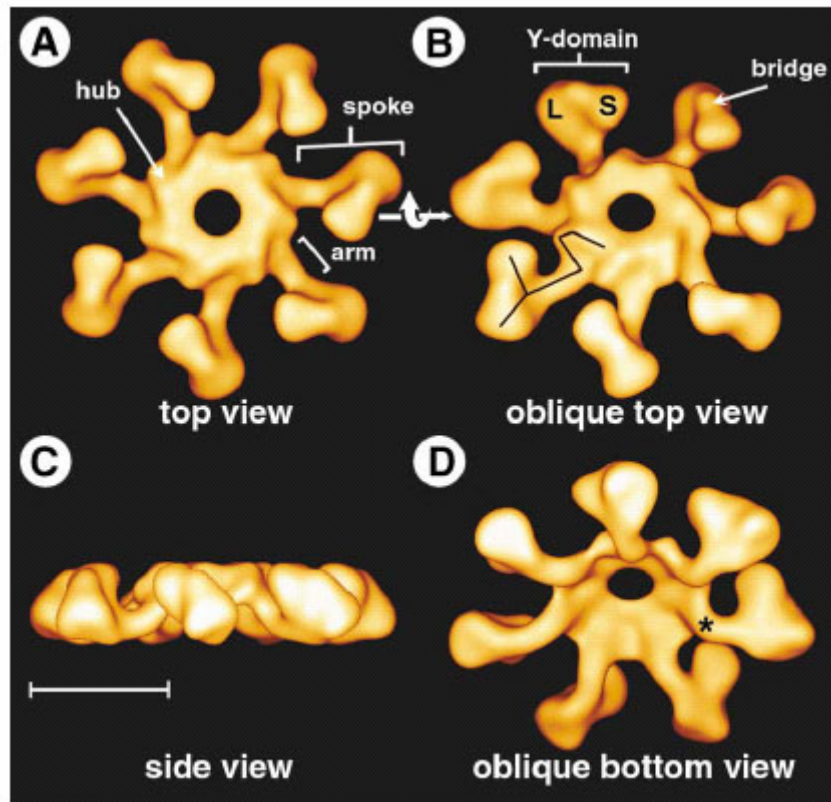


Figure 1-6. Three-Dimensional Structure of the Apoptosome

The final 3D structure of the apoptosome from all CTF-corrected particles is shown as a series of surface views that are related by rotations about the horizontal arrow. (A) The apoptosome is shown in a top view along the 7-fold symmetry axis. Features of interest are labeled, including the central hub, the spoke, and the arm. (B) Details of the spoke are evident in an oblique top view. They include the Y domain with two lobes that are marked large (L) and small (S). A bridge is located between the two lobes. By varying the threshold, we delineated the most likely path for an Apaf-1 monomer by tracing the regions with strongest connectivity within the hub (see Y-shaped black line). (C) A side view of the apoptosome reveals the unusual axial ratio of this particle. The scale bar is 100 Å. (D) An oblique bottom view shows the pucker of the particle. The arms are bent at an elbow (see asterisk) located proximal to the hub. (Adopted from Acehan et al., 2002)

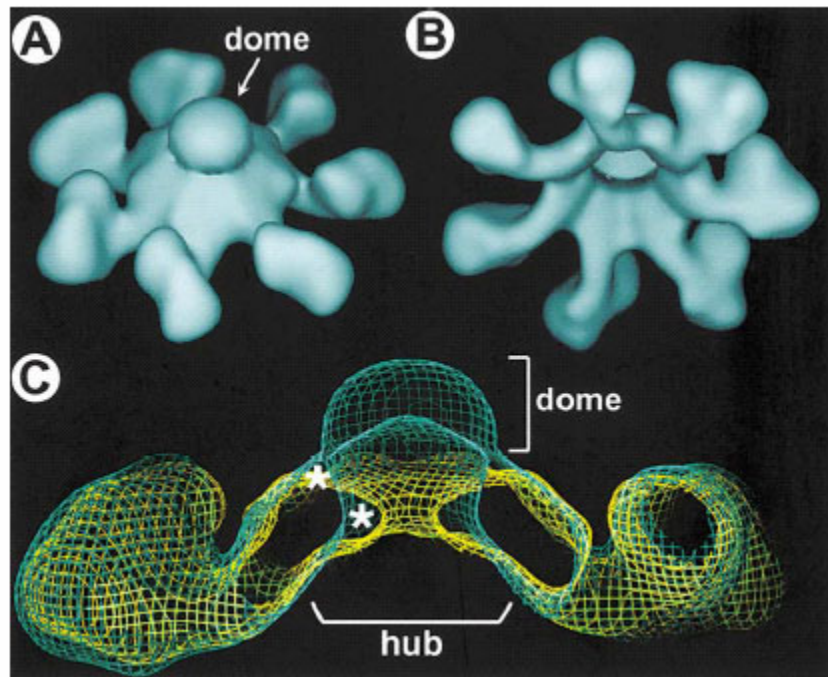


Figure 1-7. 3D Structure of the Apoptosome with Bound Procaspase-9

(A) An oblique top view is shown of the apoptosome with bound procaspase-9. A central dome-like feature is present on the hub. (B) A bottom oblique view suggests that the concave surface of the procaspase-9 complex is similar to the apoptosome without procaspase-9. (C) Density maps for the apoptosome (in yellow) and the procaspase-9 apoptosome (in green) were aligned in "O." A central slab of density suggests that the hub may have an altered conformation when procaspase-9 is bound. This conformational change involves an upward movement of the putative Apaf-1 CARD (see asterisks) and results in a larger diameter for the central pore. (Adopted from Acehan et al., 2002)

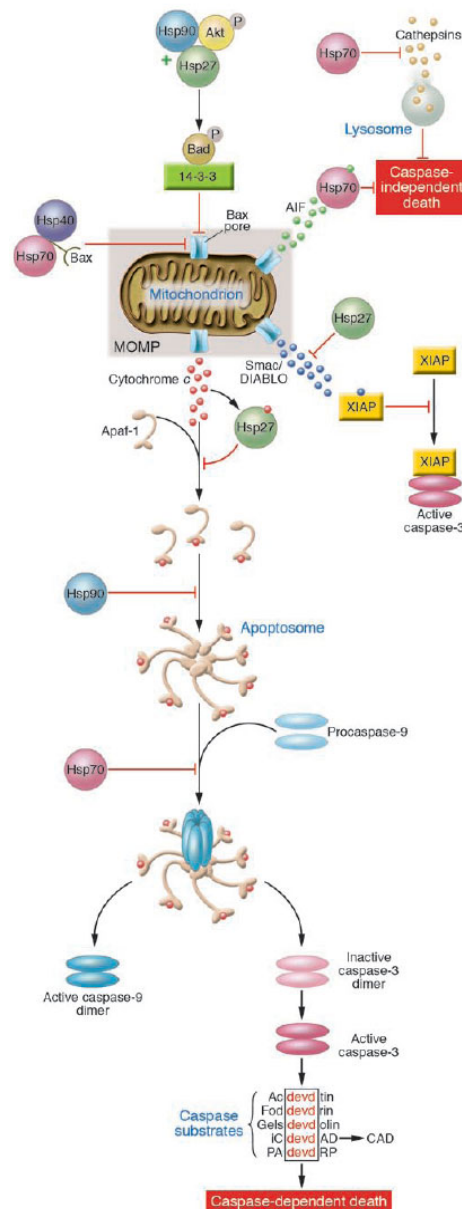


Figure 1-8. Regulation of the intrinsic pathway by Hsps.

Hsps regulate several aspects of the intrinsic apoptotic pathway. These include both direct mediators — e.g., Bax — and indirect regulators — e.g., Akt — of mitochondrial membrane permeabilization to prevent MOMP as well as events downstream of mitochondrial disruption to regulate apoptosome assembly. Caspase-independent cell death may also be affected via Hsp-mediated suppression of AIF activity and inhibition of lysosome permeabilization and cathepsin release. (Adopted from Beere, 2005)

Chapter 2 : Distinctive Roles of PHAP Proteins and Prothymosin- α in a Death Regulatory Pathway

(This work was led by Dr. Xuejun Jiang. It was published in Science 299 (5604); 223-226. My contribution in this study is summarized in Figure 5.)

Abstract

A small molecule, α -(trichloromethyl)-4-pyridineethanol (PETCM), was identified by high-throughput screening as an activator of caspase-3 in extracts of a panel of cancer cells. PETCM was used in combination with biochemical fractionation to identify a pathway that regulates mitochondria-initiated caspase activation. This pathway consists of tumor suppressor putative HLA-DR-associated proteins (PHAP) and oncoprotein prothymosin- α (ProT). PHAP proteins promoted caspase-9 activation after apoptosome formation, whereas ProT negatively regulated caspase-9 activation by inhibiting apoptosome formation. PETCM relieved ProT inhibition and allowed apoptosome formation at a physiological concentration of deoxyadenosine triphosphate (dATP). Elimination of ProT expression by RNA interference sensitized cells to ultraviolet irradiation-induced apoptosis and negated the requirement of PETCM for caspase activation. Thus, this chemical-biological

combinatory approach has revealed the regulatory roles of oncoprotein ProT and tumor suppressor PHAP in apoptosis.

Introduction

Cytochrome *c* release from mitochondria to the cytosol marks a defined moment in a mammalian cell's response to a variety of apoptotic stimuli, in which the normal electron transfer chain is disrupted and caspases become active (1, 2). The released cytochrome *c* readily binds to apoptotic protease activating factor 1 (Apaf-1) and induces a conformational change that allows stable binding of deoxyadenosine triphosphate/adenosine triphosphate (dATP/ATP) to Apaf-1, an event that drives the formation of a heptamer Apaf-1-cytochrome *c* complex called the apoptosome (Goldstein et al., 2000; Jiang and Wang, 2000). The apoptosome recruits and activates procaspase-9, which in turn activates the downstream caspases such as caspase-3, -6, and -7 (Li et al., 1997; Acehan et al., 2002). These caspases cleave many intracellular substrates, ultimately leading to cell death (Rodriguez and Lazebnik, 1998).

The mitochondrial caspase activation pathway is tightly regulated. One major regulatory step is at the release of cytochrome *c* from mitochondria, a process controlled by the Bcl-2 family of proteins (Adams and Cory, 1998; Chao and Korsmeyer, 1998). The inhibitors of apoptosis (IAP) also regulate

this pathway by directly inhibiting caspase activity (Jiang and Wang, 2000; Deveraux and Reed, 1999). IAP proteins are antagonized by mitochondrial proteins such as Smac/Diablo and Omi/HtrA2 after they are released to cytoplasm (Du et al, 2000; Verhangen et al, 2000 and 2001; Suxuki et al., 2001; Hegde et al., 2002).

We have identified a death regulatory pathway by using a combined high-throughput chemical screen and biochemical fractionation approach. The pathway consists of tumor suppressor PHAP proteins and the oncoprotein ProT, each playing a distinctive role in regulating apoptosome formation and activity.

Results and Discussions

PETCM stimulates apoptosome formation and caspase-3 activation.

Caspase-3 in HeLa cell extracts can be activated by the addition of 1 mM dATP through the mitochondria caspase activation pathway (Liu et al., 1996). To screen for small molecules that activate caspases, we screened 184,000 compounds for caspase-3 activators with HeLa cell extracts (S-100 fraction). The most potent positive hit from this large-scale screen was

PETCM (Fig. 1A). This molecule has a simple chemical structure with no resemblance to dATP.

Addition of PETCM to the S-100 fraction in the absence of exogenous dATP activated caspase-3 in a dose-dependent manner measured by the liberation of colorimetric artificial caspase-3 substrate (Fig. 1B). The effective concentration for caspase-3 activation is between 0.1 and 0.2 mM. At 0.2 mM, PETCM was more efficient in activating caspase-3 than 1 mM dATP (Fig. 1C). In addition, cell extracts from many human cancer lines, including colon cancer, prostate cancer, promyelocytic leukemia, T cell leukemia, bone marrow leukemia, malignant melanoma, lymphoma, and glioblastoma cells, were responsive to PETCM (Jiang et al., data not shown).

To determine how this small molecule promotes activation of caspase-3, we analyzed apoptosome formation by gel-filtration chromatography (Fig. 1D). Apaf-1 in a normal HeLa cell S-100 fraction was mostly in an inactive monomeric form. After incubating with 1 mM dATP, most of the Apaf-1 shifted to a size of ~1 million daltons, indicating apoptosome formation. After the S-100 fraction was incubated with 0.2 mM PETCM, Apaf-1 exhibited a similar shift. The efficiency of apoptosome formation was better with 0.2 mM PETCM, which is consistent with the caspase-3 assay result (Fig. 1C).

Stimulatory activity of PHAP proteins in the PETCM-initiated caspase activation pathway.

To determine how PETCM promotes apoptosome formation and caspase-3 activation, we further fractionated HeLa cell extracts with an anion-exchange column to search for proteins that mediate the PETCM effect. We obtained three fractions. The first fraction, Q-ft, flew through the column and contained cytochrome *c* (Liu et al., 1996); the second fraction, Q30, eluted with 0.3 M NaCl and contained Apaf-1 (Zou et al., 1997) and procaspase-9 (Li et al., 1997); the third fraction, Q100, eluted with 1 M NaCl. When we incubated all three fractions together in the presence of 10 μ M dATP, the physiological concentration in cells, we observed little caspase-3 activation (Fig. 2A). In contrast, when we added 1 mM dATP, we observed robust caspase-3 activation. In the presence of 0.2 mM PETCM, we observed caspase-3 activation at 10 μ M dATP, indicating that the combination of these three fractions mimicked what happened in the S-100 fraction. We observed no caspase-3 activation if we omitted dATP, indicating that PETCM function still requires dATP. As for the cell extracts (Fig. 1), the endogenous nucleotide was sufficient to support caspase-3 activation by PETCM. Omitting the Q-ft (cytochrome *c*) or Q30 (Apaf-1/procaspase-9) fraction diminished the caspase-3 activating activity of PETCM. Surprisingly, omitting the Q100 fraction also

reduced caspase-3 activating activity (Fig. 2A), suggesting that this fraction contained an unknown protein factor(s) that mediated the stimulating effect of PETCM.

The stimulatory activity in the Q100 fraction was purified by chromatography (Fig. 2, B and C). For the final Mono Q column, a single activity peak at fractions 22 to 24 correlated with three proteins of 32, 29, and 35 kD. We identified these three proteins by mass spectrum analysis as putative HLA-DR-associated protein-1 (PHAPI, also called PP32 and LANP) (Vaesen et al., 1994; Chen et al., 1996; Matilla et al., 1997), PHAPI2a (also called SSP29 and April) (Zhu et al., 1997; Mencinger et al., 1998), and a theoretical protein in the National Center for Biotechnology Information database, which we named PHAPIII. The amino acid sequences of the three proteins are more than 80% identical (fig. S1). They have a long acidic COOH-terminus and a leucine-rich region in the middle (fig. S1). In mammalian cells, PHAP proteins are putative tumor suppressors (Chen et al., 1996; Brody et al., 1999; Bai et al., 2001), a function consistent with the proapoptotic activity identified here.

ProT inhibits caspase-3 activation and PETCM antagonizes the inhibitory activity.

Surprisingly, the stimulatory effect of PHAP proteins on caspase-3 activation was independent of PETCM (Fig. 3A). However, when the Q100 fraction, from which the PHAP proteins were purified, was also added, the stimulatory activity of the PHAP proteins was suppressed. PETCM reversed the suppression. This suggested that there was an inhibitory factor in the Q100 fraction as well. The PHAP proteins functioned only when the inhibitory factor was antagonized by PETCM. We purified a single inhibitory activity (Fig. 3, B and C) and identified it by mass spectrum analysis as the oncoprotein ProT (Dosil et al., 1993, Orre et al., 2001).

ProT and PHAP distinctively regulate apoptosome formation and activity.

Recombinant PHAPI stimulated caspase-3 activation when added to the Q30 fraction plus cytochrome *c* and 10 μ M dATP. The activity was inhibited when we included recombinant ProT in the reaction mixture, and the inhibitory effect of ProT was reversed in the presence of PETCM (Fig. 4A). In the presence of ProT, formation of apoptosome was efficiently blocked, and PETCM relieved this effect (Fig. 4B). In contrast, the presence of PHAPI did not affect the efficiency of apoptosome formation. Instead, we observed more activated caspase-9, and increased caspase-9 was associated with apoptosome (Fig. 4C). Pull-down experiments also showed more association of active

caspase-9 with Apaf-1 in the presence of PHAPI (Jiang et al., data now shown). These results indicate that ProT and PHAP regulate caspase-3 activation at different steps. ProT inhibits caspase-3 activation by blocking apoptosome formation and therefore acts more upstream in this regulatory pathway; PHAPI does not affect apoptosome formation but accelerates its activity to promote more caspase-9 activation. PETCM promotes caspase-3 activation by removing the inhibition of ProT on apoptosome formation, allowing PHAPs to stimulate apoptosome activity. Interestingly, the PETCM effect cannot be reproduced in a reconstituted system containing purified Apaf-1, procaspase-9, cytochrome *c*, PHAP, and ProT. Therefore, an additional factor(s) present in the Q30 fraction is required (Jiang et al., data now shown).

Elimination of ProT in vivo sensitizes HeLa cells to an apoptotic stimulus and bypasses PETCM action.

To verify the apoptotic roles of PHAP and ProT in vivo, we used RNA interference (RNAi) to eliminate their expression in cells. RNAi against PHAP proteins was not successful, possibly because there are multiple forms of PHAP and they are stable proteins. RNAi against ProT did efficiently eliminate the ProT messenger RNA (mRNA) (Fig. 5A). Under this condition, we observed no apoptosis. However, when irradiated with ultraviolet (UV)

light, the cells treated with ProT RNAi showed a higher rate of apoptosis (Fig. 5B). Twelve hours after UV irradiation, more than 70% of the ProT RNAi-treated cells showed apoptotic morphology, whereas control RNAi-treated cells showed only 25% cell death. Cell death correlated with the caspase-3 activation as higher caspase-3 activity was also observed in the ProT RNAi-treated cells (Fig. 5C). The RNAi experiment also confirmed that PETCM functions to antagonize the inhibitory activity of ProT (Fig. 5D). Cell extracts from control RNAi-treated cells were responsive to PETCM. In contrast, cell extracts from ProT RNAi-treated cells activated caspase-3 independently of PETCM.

ProT and PHAP as apoptotic regulators.

ProT is an oncoprotein required for cell proliferation (Dosil et al., 1993; Orre, 2001; Sburlati, 1991; Pineiro, 2000; Smith, 1993; Rodriguez, 1998; Magdalena, 2000; Wu, 1997; Eiler, 1991). However, the biochemical mechanism for the oncogenic property of ProT was not clear (Pineiro et al., 2000). Our data indicate that one of the biochemical functions of ProT is to prevent apoptosome formation. Such a biochemical activity is consistent with its oncogenic function, because other previously known negative regulators of apoptosis such as Bcl-2 (Adams and Cory, 1998; Chao and Korsmeyer, 1998)

and IAPs (Deveraux and Reed, 1999) have been shown to have oncogenic activities as well. The inhibition of apoptosome formation by ProT also offered an explanation for a long-standing puzzling observation that up to a millimolar concentration of dATP is required to trigger efficient caspase-3 activation *in vitro*. The intracellular dATP under normal conditions is in the 10- μ M range and does not arise during apoptosis (Mesner et al., 1999). The requirement for millimolar dATP also contradicts the direct binding studies with purified Apaf-1 and dATP. In this study, the dissociation constant of dATP binding to Apaf-1 is at the micromolar level in the presence of cytochrome *c*, and micromolar amounts of dATP also efficiently stimulate caspase-3 activation in a reconstituted system containing purified Apaf-1, procaspase-9, and cytochrome *c* (Jiang and Wang, 2000). It is clear now that most dATP is probably used for repressing ProT in HeLa cell S-100. When ProT is suppressed by PETCM, 10 μ M dATP is enough to trigger apoptosome formation and PHAP can subsequently accelerate the activity of the machinery.

Unlike ProT, PHAP proteins function as tumor suppressors in mammalian cells to inhibit cell growth (Vaesen et al., 1994; Brody et al., 1999; Bai et al., 2001). They have been shown to inhibit protein phosphatase 2A (Li, Makkinje and Damuni, 1996) and block histone acetylase (Seo et al., 2001). How these biochemical functions are linked to its cellular antigrowth function

is not clear. But, in light of our finding that PHAP proteins promote apoptosis by accelerating caspase-9 activation, we suggest that it may inhibit cell growth by promoting apoptosis. Interestingly, PHAP can interact with ataxin-1, a protein that is mutated in the neural degenerative disease spinocerebellar ataxia type 1 (Matilla et al., 1997). This suggests a role of PHAP in the disease. Further, certain PHAP proteins are preferentially expressed in mouse cerebellum during its most active developmental period characterized by massive apoptosis (Matsuoka et al., 1994; Mutai et al., 2000; Radrizzani, 2001). Because apoptosis and Apaf-1 are essential in this early brain developmental stage (Cecconi et al., 1998; Toshida et al., 1998), we suggest that PHAP, a stimulator of apoptosome activity, might also play a crucial role during brain development, a readily testable model.

Experimental Procedures

General Methods and Materials

Nucleotide dATP was purchased from Pharmacia. Horse heart cytochrome *c* was purchased from Sigma. Colorimetric and fluorogenic caspase-3 peptide substrates were from CalBiochem. Polyclonal anti-Apaf-1 antibody was prepared as described previously (H. Zou, Y. Li, X. Liu, X.

Wang, J. Biol. Chem. 274, 11549 (1999).). Anti-caspase-9 antibody (#9505) was purchased from Cell Signaling. All the cell lines were purchased from ATCC. Protein concentration was determined by the Bradford method. General biochemical and molecular biology methods were performed as described in Molecular Cloning (Sambrook et al., 1989).

High Throughput Screening (HTS) protocol for caspase-3 activators

The HTS screen was essentially a cell-lysate assay in which the endpoint, activation of caspase-3, was monitored by the cleavage of a colorimetric substrate. HeLa cell lysate was prepared by Cellex Bioscience. This lysate was thawed and centrifuged before use (15K rpm in a JA20 Beckman rotor). The lysate was diluted (to 30% final concentration) with a buffer that contained Ac-DEVD-pNA (250 μ M final), dATP (100 μ M final), DTT (2 mM final); 50 μ l of this material was immediately added to plates that contained 12 compounds per well (dried, 20 μ M final per compound), and an initial absorbance was read at 390 nm.

The plates were allowed to incubate for three to four hours. When 90% of the Ac-DEVDpNA was converted by the activated capsase-3 in the control plate, the screening plates were read again at 390 nm. The change in absorbency was scaled to the fully-activated control (cytochrome *c*) and the negative control (no compound). Wells that exhibited greater than 5%

activation were investigated further in the same assay to elucidate the active compounds. An archived collection of 184,000 small organic molecules derived from the Abbott in-house synthetic efforts supplemented with commercially available compounds were screened in this manner. Of these, twenty-eight compounds were identified as having some stimulating effect in the assay. Of these, six had measurable EC₅₀'s, with PETCM being the most active compound.

Colorimetric assay for caspase-3 activity

In a 20- μ l system, 40 μ g HeLa S-100 was incubated with indicated amount of PETCM and 0.2 mM colorimetric DEVD substrate (Calbiochem). Samples were applied to a 384- well microplate, the reaction was carried out at 30 oC, and OD405 was measure by Xfluo4 spectrometry reader (TECAN Austria).

Colorimetric assay for caspase-3 activity

In a 20- μ l system, 40 μ g HeLa S-100 was incubated with indicated amount of PETCM and 0.2 mM colorimetric DEVD substrate (Calbiochem). Samples were applied to a 384- well microplate, the reaction was carried out at 30 oC, and OD405 was measure by Xfluo4 spectrometry reader (TECAN Austria). with 10-ml of Buffer A containing 300 mM NaCl, and the eluted protein peak (~ 4 ml) was collected (Q30). Subsequently, the column was

eluted with Buffer A containing 1 M NaCl, and the protein peak (~ 3 ml) was collected and dialyzed for overnight (Q100).

Purification and identification of PHAP from HeLa S-100

All purification steps were carried out at 4 °C, and chromatography was performed on a Pharmacia FPLC system. HeLa cell S-100 was prepared in Buffer A containing protease inhibitors as described (Liu et al., 1996). About 150 ml of HeLa S-100 (~ 1 g total protein) was obtained from 25 liters of cell culture. The HeLa S-100 was applied to a Q-Sepharose column (40-ml bed volume) equilibrated with Buffer A. After washing the column with 250 ml of Buffer A containing 0.3 M NaCl, the stimulatory activity was eluted with Buffer A containing 1 M NaCl and the eluted protein peak was collected (100 ml, ~ 125 mg total protein). After adjusting NaCl concentration to 4 M by dissolving NaCl powder, it was loaded on a phenyl-Sepharose column (40-ml bed volume) equilibrated with Buffer A containing 4 M NaCl. The activity flew through the column (~ 6 mg total protein). After adjusting $(\text{NH}_4)_2\text{SO}_4$ concentration to 60% saturation, it was applied to a 1-ml phenyl-sepharose column equilibrated with Buffer A containing 60% saturated $(\text{NH}_4)_2\text{SO}_4$, and the activity was eluted with a gradient from 60% to 20% saturated $(\text{NH}_4)_2\text{SO}_4$ in 40 ml of Buffer A. The activity was combined (~ 0.7 mg total protein), concentrated to 0.5 ml, and subsequently resolved by a 25-ml Superdex 200

gel filtration column with Buffer A containing 50 mM NaCl. The active fractions were combined (~ 0.45 mg total protein), and finally resolved by a Mono Q 5/5 column with a 300-600 mM NaCl gradient in 40 ml of Buffer A. The activity was eluted at about 500 mM NaCl. The purified proteins were identified as PHAPI and related proteins by Mass-Mass spectrum analysis at Cell Signaling Alliance Facility at UT Southwestern Medical Center according to standard procedures.

Purification and identification of ProT from HeLa S-100

All purification steps were carried out at 4 °C, and chromatography was performed on a Pharmacia FPLC system. One hundred liters of HeLa cell culture was used to obtain 600 ml of HeLa S100 (~ 3.6 g total protein). Ammonium sulfate concentration was adjusted to 70% saturation, and the precipitated protein was removed by centrifugation. The supernatant (~ 0.6 g total protein) was loaded on a phenyl-Sepharose column (40-ml bed volume) equilibrated with Buffer A containing 70% saturated $(\text{NH}_4)_2\text{SO}_4$. After washing the column with 250 ml of Buffer A containing 70% saturated $(\text{NH}_4)_2\text{SO}_4$, the inhibitory activity was eluted with Buffer A containing 30% saturated $(\text{NH}_4)_2\text{SO}_4$ and the eluted protein peak was collected (100 ml, ~ 60 mg total protein). The activity was dialyzed against Buffer A for overnight and loaded on a 8-ml Mono-Q equilibrated with Buffer A, and subsequently eluted

with a gradient of 300 – 600 mM NaCl in 100 ml of Buffer A. The active fractions were combined (~ 1.2 mg total protein), and loaded on a 2-ml hydroxyapatite column equilibrated with Buffer A. A gradient of 0 – 100 mM KPO₄ (pH 7.5) in 20 ml of Buffer A was performed to elute the inhibitory activity. The active fractions were combined (~ 0.4 mg protein), concentrated to 1 ml, and subjected to 2 runs of gel filtration on a Superdex 200 column eluted with Buffer A. The active fractions were combined (~ 0.2 mg), and resolved by a 1-ml Mono-Q column with a gradient of 300 – 600 mM NaCl in 30 ml of Buffer A. The purified protein was identified as prothymosin- α by Mass-Mass spectrum analysis at Cell Signaling Alliance Facility at UT Southwestern Medical Center according to standard procedures.

Cloning of PHAPI and ProT, and production of recombinant proteins

PHAPI open reading frame (ORF) was amplified by PCR from image clone AA488559 (Incyte Genomics Inc.) using primers CGGCAGATCTCTGGATCCATGGAGATGGGCAGACGGATTC and CGCCGTCGACTTAGTCATCATCTTCTCCCTC. The amplified product was subcloned into BamHI/SalI sites of pET-28a(+) vector (Novagen). The plasmid was used to express recombinant His-tagged PHAPI in BL21(DE3) strain and the protein was purified using NTA-agarose (Qiagen) followed by Q-Sepharose chromatography. ProT ORF was amplified by PCR from image

clone B315161 (Incyte) using primers CCGGCATATGTCAGACGCAGCCGTAGAC and CCGGCTCGAGGTCATCCTCGTCGGTCTTCTG. The amplified product was subcloned into NdeI/XhoI sites of pET-21b vector (Novagen). The plasmid was used to express recombinant Histagged ProT in BL21(DE3) strain and the protein was purified using NTA-agarose (Qiagen) followed by Q-Sepharose chromatography.

RNAi of ProT and cell death analysis of HeLa cells

Double-strand siRNA UCACCACCAAGGACUUAAA, corresponding to a region of ProT mRNA, with dTdT overhang in the 3'-end, was synthesized by Dharmacon to disrupt ProT mRNA in HeLa cells. Double-strand siRNA GCAGCACGACUUCUUCAAGU (3'-end dTdT overhang) corresponding to a region of green fluorescence protein (GFP) was used as a control. DNA primers ATGATCTCGGATGACCAAAC and GAGGCGGCTGCGGCGAGCA were used to measure ProT mRNA by RT-PCR. DNA primers TCCACCACCCTGTTGCTGTA and ACCACAGTCCATGCCATCAC were used for RT-PCR of GAPDH. HeLa cells were grown in 6-well plates. Transfection of siRNA to HeLa cells was performed using OligofectAmine reagent (Invitrogen) according to standard procedure, the final siRNA concentration of the transfection was 16 nM. Two days after transfection, RT-

PCR was performed to measure ProT mRNA level, cells were treated with 10 mJ/cm² of UV light using UV Stratalinker 1800 (Stratagene), and cell death was accessed at indicated time. Dead cells were stained by Hoechst 33342 and counted under microscope. For caspase-3 activity measurement, cells were harvested with or without UV treatment as indicated, and lysed in Buffer A containing protease inhibitors by three cycles of freeze-and-thaw, the measurement was performed in a 100- μ l system containing 10 μ M DEVD fluorogenic substrate (CalBiochem) and 20 μ g cytosolic protein at 30 °C using a Xfluor4 spectrometry reader (TECAN Austria).

Figure 1.

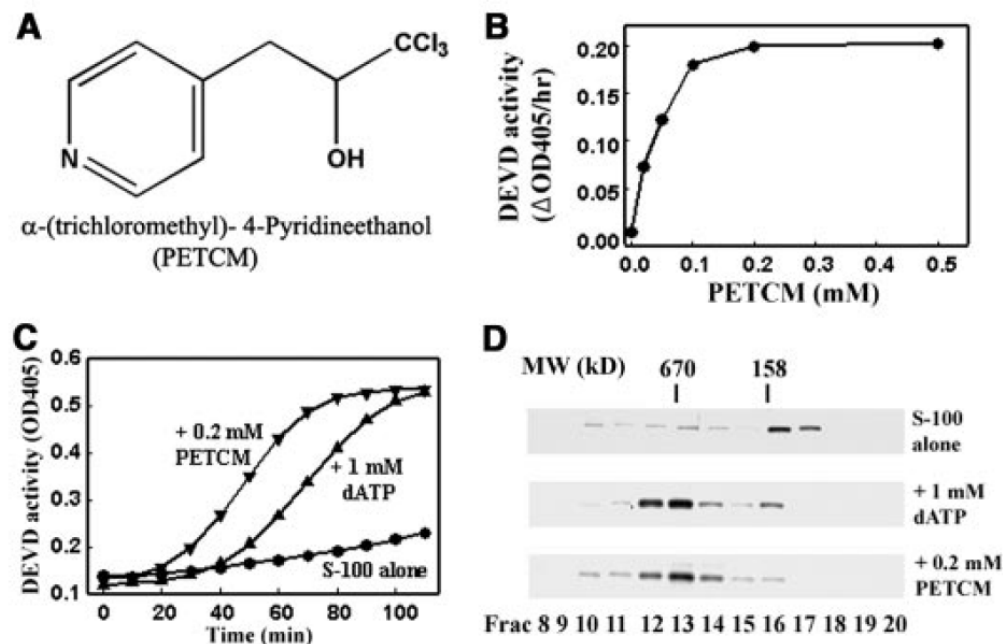


Fig. 2-1. PETCM stimulates caspase-3 activation and drives apoptosome formation in HeLa cell cytosol. (A) Structure of PETCM. (B) PETCM stimulates caspase-3 activity (DEVD activity) of HeLa S-100 in a dose-dependent manner. The colorimetric assay for caspase-3 activity was performed as described (18). (C) Time course comparison of the stimulatory effects of PETCM and dATP. PETCM and dATP were added as indicated. (D) PETCM drives apoptosome formation. HeLa S-100 was incubated with 1 mM dATP or 0.2 mM PETCM as indicated at 30°C for 1 hour. Mixtures were then resolved with a Superose 6 gel-filtration column. The column fractions were subjected to SDS-polyacrylamide gel electrophoresis and Apaf-1 in each fraction was detected with an immunoblot against Apaf-1.

Figure 2.

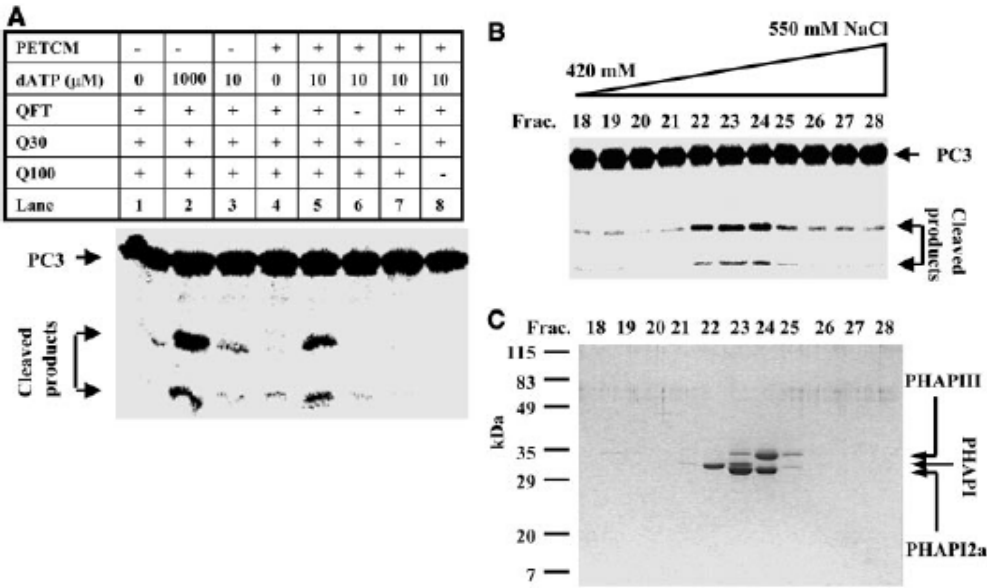


Fig. 2-2. Identification of a stimulatory activity to mediate PETCM effect. (A) Fractions Q-ft, Q30, and Q100 were prepared (18), and the PETCM effect was examined with the fractions as follows. Fractions were mixed and different amounts of dATP and/or 0.2 mM PETCM were added as indicated. The reactions were carried out at 30°C for 1 hour. Caspase-3 activation of each mixture was measured by cleavage of [35S]methionine-labeled caspase-3 substrate, as described in (16). Procaspase-3 (PC3) and the cleaved products are marked by arrows. (B) Purification of stimulatory activity. Purification was performed as described (18). Activity of fractions from the final Mono Q column was assayed as follows. In a 20- μ l system, 3 μ l of Q30, 100 nM cytochrome *c*, 10 μ M dATP, and 0.2 mM PETCM were mixed in buffer A, and 2 μ l of each fraction was added as indicated. Caspase-3 activation of each mixture was measured as cleavage of PC3. (C) The final Mono Q fractions (30 μ l each) were resolved by SDS-polyacrylamide gel electrophoresis and the gel was stained with silver. The three purified proteins, PHAPI, PHAPI2a, and PHAPIII, are indicated.

Figure 3.

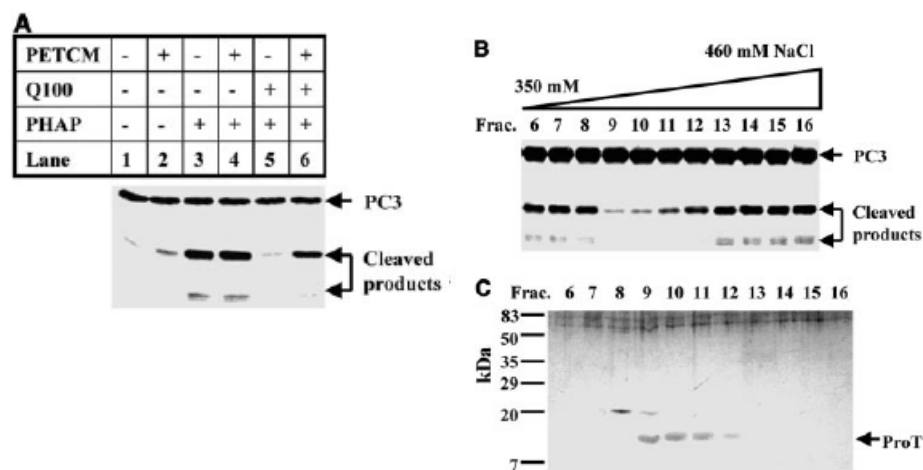


Fig. 2-3. Purification of inhibitory activity in the Q100 fraction. (A) Inhibitory activity in the Q100 fraction. The Q30 fraction, 100 nM cytochrome *c*, and 10 μ M dATP were mixed, and PHAP, the Q100 fraction, and/or PETCM were added as indicated. Caspase-3 activation of each mixture was measured as cleavage of procaspase-3 (PC3). (B) Purification of inhibitory activity. Purification was performed as described in (18). Activity of fractions from the final Mono Q chromatography was assayed as follows. The Q30 fraction, 100 nM cytochrome *c*, 10 μ M dATP, and 2 μ l of purified PHAP were mixed, and 4 μ l of each fraction was added as indicated. Caspase-3 activation of each mixture was measured as cleavage of PC3. (C) The final Mono Q fractions (10 μ l each) were resolved by SDS-polyacrylamide gel electrophoresis and the gel was stained with silver.

Figure 4.

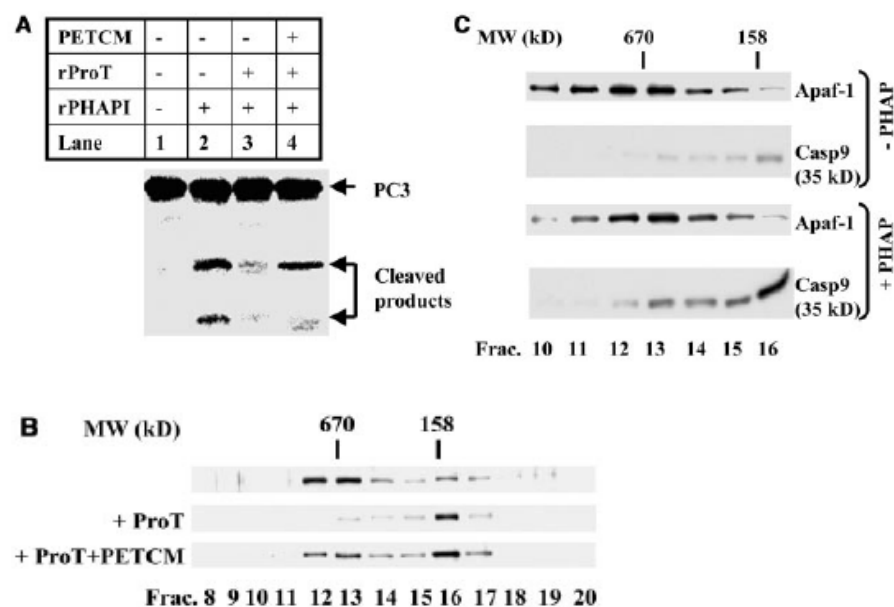


Figure 5.

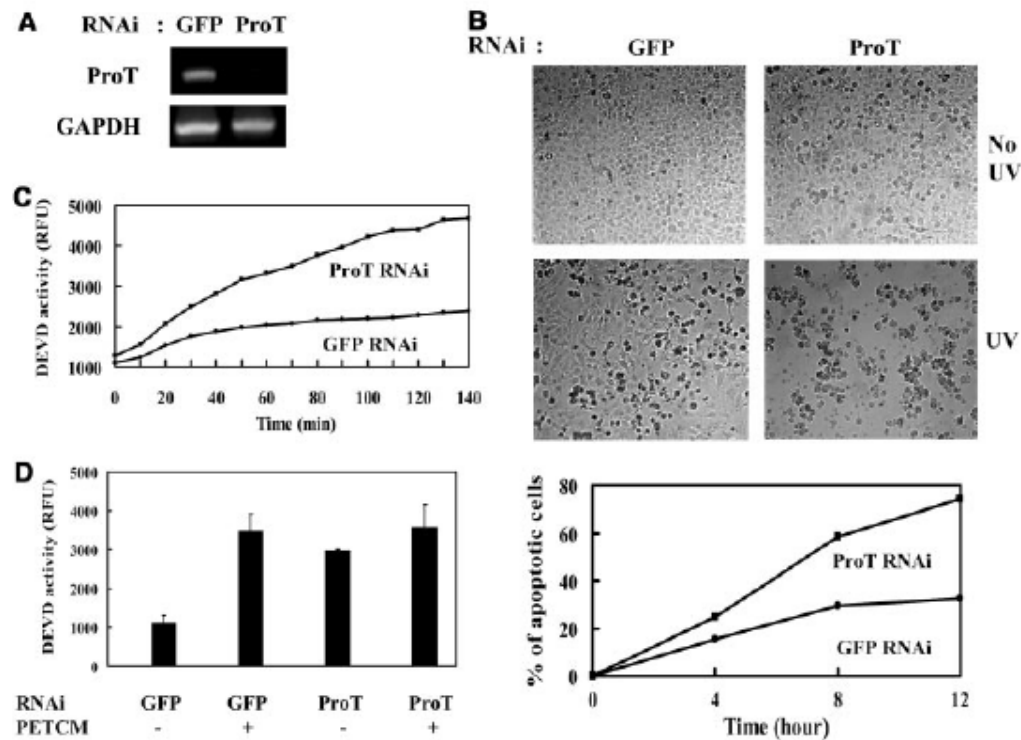


Fig. 2-5. Elimination of ProT by RNAi-sensitized UV-induced apoptosis in HeLa cells. (A) Reverse transcriptase polymerase chain reaction (RT-PCR), showing elimination of ProT messenger by RNAi. Two days after transfection with ProT small interfering RNA (siRNA) or green fluorescent protein (GFP) siRNA (18), RT-PCR of ProT was performed. RT-PCR of glyceraldehyde phosphate dehydrogenase (GAPDH) was used as the control. (B) ProT RNAi sensitizes UV-induced cell death. Cells were treated with ProT or GFP RNAi. Top panel: Micrographs without UV treatment or 12 hours after UV irradiation. Bottom panel: Cell death counting with Hoechst staining at the indicated times after UV irradiation. (C) ProT RNAi increases UV-induced caspase-3 activation. Cells were treated with ProT or GFP RNAi and harvested 8 hours after UV irradiation. Caspase-3 activity in the S-100 of RNAi-treated cells was measured by the fluorogenic caspase-3 assay (18). (D) Elimination of ProT by RNAi negates the PETCM requirement for caspase-3 activation. HeLa cells were transfected with ProT siRNA or GFP siRNA as indicated. After 2 days, cells were harvested and caspase-3 activity of the cell lysate was measured after 2 hours of incubation at 30°C in the presence or absence of 0.2 mM PETCM as indicated. All the experiments were done at least three times with similar results.

Figure S1.

```

PHAPI      1 MEMCRRHLELRNRTFSDVKEVLVDNERSNEGKLEGLTDEFESLEFLSTINVGLTSIANL
PHAPI2a    1 MDMKRRHLELRNRTFAVRELVLVDNCKSNDGKIEGLTAEFVNLEFLSLINVGLISVSNL
PHAPIIII   1 MEMKKRIHLELRNRSPEEVHLEVLVDNCLCVNGEIEGLNDTFKELEFLSMANVELSSLARL

PHAPI      61 PKLNKLRKLELSDNRVSGGLEVLAEKCPNLTHNLSCGNKIKDLSITIEPLKKLENLKSDDL
PHAPI2a    61 PKLLEKLRKLELSDNRIFGGGLDLAEKCPNLTHNLSCGNKIKDLSITIEPLKKLELKSDDL
PHAPIIII   61 PSLNKLRLKLELSDNRIISGGLEVLAEKCPNLTHNLSCGNKIKDLSITIEALQNLKLENLKSDDL

PHAPI      121 FNCEVTNLNDYREN VFKLLPQLTYLDGYDRDDKEAPDSDAEGYVEGLDDEEDED-EEFY
PHAPI2a    121 FNCEVTNLNDYRESVFKLLPQLTYLDGYDRDDKEAPDSDAE--VDGVDEEEDDEGEDEE
PHAPIIII   121 FNCEVTNLNDYRESIFELLQITTYLDGFDQEDNEAPDSEEDDEDGDEDDEEENEAGP

PHAPI      180 DEDACVVE---DEED-EDDEEGEEDVSGDEEEDDEECYN-----DCEVDDE----
PHAPI2a    179 DEDDEDGEEEFDEEDDEEDVECEDDDEVSEEEEFGLD-----DEDED-----
PHAPIIII   181 PEGYEEEEE-EEED-EDDEDEDBAGSEIGCEEEVGLSYLMKEEIQDEEDDDYVEE

PHAPI      223 -EDDEELGEE-RCQKRKRFEDEGEDD-
PHAPI2a    227 -EDDEE-EGG-KGKRKRDEDEGEDD--
PHAPIIII   239 GEEEEEEGGLRGEKRKRDAEDDGEEDD

```

Fig. 2-S1. Protein sequence alignment of PHAP proteins. The alignment was performed using ClustalW method. The leucine-rich repeat cap (corresponding to residue 128-146 of PHAPI) are line-marked.

Chapter 3 : Formation of apoptosome is initiated by cytochrome *c*-induced dATP hydrolysis and subsequent nucleotide exchange on Apaf-1

(This work was published in PNAS, 120(49); 17545-17550).

Abstract

Apoptosis in metazoans is executed by a group of intracellular proteases named caspases. One of the caspase-activating pathways in mammals is initiated by the release of cytochrome *c* from mitochondria to cytosol, where it binds to Apaf-1 to form a procaspase-9-activating heptameric protein complex named apoptosome. We report here the reconstitution of this pathway with purified recombinant Apaf-1, procaspase-9, procaspase-3, and cytochrome *c* from horse heart. Apaf-1 contains a dATP as a cofactor. Cytochrome *c* binding to Apaf-1 induces hydrolysis of dATP to dADP, which is subsequently replaced by exogenous dATP. The dATP hydrolysis and exchange on Apaf-1 are two required steps for apoptosome formation.

Introduction

The characteristic morphological and biochemical markers of apoptotic cell death can be attributed to the activity of a group of intracellular proteins, caspases (Alnemri et al., 1996). These markers include DNA cleavage into nucleosomal fragments, chromatin aggregation, membrane blebbing, and fragmentation of apoptotic cells into small membrane vesicles named apoptotic bodies (Wyllie, 1980; Wyllie, Kerr, and Currie, 1980; Wyllie et al., 1984). These features of apoptosis allow the dead cell to be rapidly and cleanly removed through phagocytosis by neighboring cells and macrophages, and thus the inflammation response is avoided. The critical role of caspases in apoptosis has been demonstrated by genetic studies from *Caenorhabditis elegans* to mouse (Yuan et al., 1993; Chew et al., 2004; Daish et al., 2004; Kuida et al., 1996; Kuida et al., 1998; Hakem et al., 1998).

The first caspase identified, caspase-1, previously known as interleukin-1 converting enzyme (ICE), processes interleukin-1 precursor to its mature form. Several unique properties of caspase have been uncovered by the study of caspase-1 (Thornberry et al., 1992). True to all functionally characterized caspases, caspase-1 uses a cysteine residue in its active site and is synthesized as an inactive precursor that becomes activated by proteolysis or association with its respective activator molecules (Thornberry et al., 1992; Ghornberry and Lazebnik, 1998; Shi, 2002). Caspases cleave substrates after

aspartic acid residues, a signature of this group of proteases (Thornberry et al., 1992). So far, there are 14 caspases that have been found in mammalian genomes, and they function either during immune response or apoptosis (Shi, 2002).

One of the two best-characterized caspase activation pathways is initiated from mitochondria. In response to apoptotic stimuli, cytochrome *c*, a previously known component of electron transfer chain in mitochondria, gets released to cytosol where it binds to a partner protein Apaf-1 (Liu et al., 1996; Zou et al., 1997). Apaf-1 consists of three functional domains; the N-terminal caspase recruitment domain (CARD), the middle nucleotide-binding and oligomerization domain (NOD), and the C-terminal regulatory region composed of 13 WD-40 repeats (Zou et al., 1997 and 1999). This regulatory region normally keeps Apaf-1 in an autoinhibitory state and when cytochrome *c* binds to this region, Apaf-1 becomes activated in the presence of dATP or ATP (Srinivasula et al., 1998; Adrain et al., 1999; Acehan et al., 2002). The activation is accomplished through oligomerization of seven individual Apaf-1/cytochrome *c* complexes into a wheel-like heptamer, called apoptosome (Zou et al., 1999; Acehan et al., 2002).

The central ring of the apoptosome is formed by the conjugation of seven CARD and NOD domains of Apaf-1, and each of the seven spikes

extended from the central ring is made of 13 WD-40 repeats bound to one cytochrome *c* (Acehan et al., 2002).

Apaf-1 represents a family of evolutionarily conserved caspase activators. The *Drosophila* DARK/HAC-1/dApaf-1 shares the same domain structure with Apaf-1, and *C. elegans* ced4 shares homology with Apaf-1 with the caspase recruitment and nucleotide-binding and oligomerization (NOD) domains but missing the WD-40 repeats (Rodriguez et al., 2002; Kanuka et al., 1999; Zhou et al., 1999; Yuan et al., 1992). A more distantly related protein family consists of the Nod-1 like proteins in mammals and proteins encoded by disease resistance (R) genes in plants (Martinon, Burns and Tschopp, 2002; Inohara, Ogura and Nunez, 2002). These proteins share homology with Apaf-1 in the NOD domain but contain diverse protein–protein interaction domains at their N termini and mostly leucine-rich repeats at their C termini (Inohara, Ogura and Nunez, 2002). These proteins play an essential role in innate immune response, although their biochemical function has not been fully characterized.

Apaf-1-mediated caspase activation is accomplished through a cascade of caspases, with caspase-9 functioning as the initiator caspase and caspase-3 and caspase-7 as the downstream effector caspases (Li et al., 1997). Caspase-9 contains a caspase recruitment domain (CARD) domain of its own at the N

terminus through which it binds the central ring of apoptosome (Acehan et al., 2002). Once bound to apoptosome, procaspase-9 becomes activated. The Apaf-1/caspase-9 complex then works as a holoenzyme that cleaves and activates caspase-3 and caspase-7, which in turn cleave their substrates leading to apoptosis (Rodriguez and Lazebnik, 1999).

This Apaf-1-mediated caspase activation pathway absolutely requires the presence of dATP or, at higher concentration, ATP (Liu et al., 1996; Li et al., 1997). However, the precise roles of the nucleotide and cytochrome *c* are still not clear. There is also confusion on whether the binding and/or hydrolysis of nucleotide are needed and, if so, whether it plays a positive or negative role for apoptosome assembly (Zou et al., 1999; Jiang and Wang, 2000; Riedl et al., 2005). Here we report the detailed biochemical analysis of this caspase-activating pathway addressing the above mentioned unresolved issues.

Results

Reconstitution of Caspase-3 Activation Using Purified Protein Components.

As shown in Fig. 1A, we have generated and purified recombinant human Apaf-1, procaspase-9, and procaspase-3 from insect cells by using

baculovirus expression system. It is worth mentioning that although we were able to generate recombinant Apaf-1 before, we did it with a pool of Apaf-1 cDNAs instead of a clone (Zou et al., 1997); we had to use this method because the 13 WD-40 repeat sequences at the 3' end of Apaf-1-coding region were prone to recombination when the plasmid was replicated in bacteria. Therefore, the plasmid prepared from bacteria grown from a single colony was always a mixture resulted from DNA recombination. To circumvent this problem, we pooled bacterial colonies soon after they appeared on agar plates to minimize the time for recombination. However, after several rounds of propagation, the baculovirus vector containing Apaf-1 cDNA became heterogeneous, and the protein yield was poor. We noted that recombination did not happen if we kept the bacteria-hosting Apaf-1 encoding plasmid under 16°C at all time. We then used this strategy to reclone Apaf-1 ORF, correct all of the mutations, and use it for making Apaf-1 protein in SF21 insect cells. Now, we routinely make up to 10 mg of purified Apaf-1 protein from a liter of SF21 cell culture, and the purified protein was used throughout this study.

As shown in Fig. 1 B and C, when purified Apaf-1, procaspase-9, procaspase-3, and cytochrome *c* were mixed in the absence of nucleotide, there was no caspase-9 and caspase-3 activation as measured by their cleavage (lane

1). In contrast, in the presence of 10 μ M dATP, most of caspase-9 and caspase-3 were activated after incubation (lane 2).

Preincubation of Apaf-1 and Cytochrome *c* Without dATP Inactivates Apaf-1.

The nucleotide requirement was observed early for cytochrome *c*-induced caspase-3 activation (Liu et al., 1996). However, surprisingly, when Apaf-1 and cytochrome *c* were preincubated without dATP, they became permanently inactivated, and subsequent addition of dATP was not able to recover the activity (Fig. 1 B and C, lane 3). On the other hand, preincubating Apaf-1 and cytochrome *c* separately did not affect their activity at all (Fig. 1D). This finding indicated that Apaf-1 underwent irreversible changes when incubated with cytochrome *c* in the absence of dATP.

Other than dATP, ATP is able to support Apaf-1/cytochrome *c*-mediated caspase activation when used at higher concentrations (Li et al., 1997; Jiang and Wang et al., 2000). Moreover, the 5'-triphosphate metabolite of clinically used chemotherapeutic drugs 2-chloro-2'-deoxyadenosine (2CdA, cladribine) and 9--D-arabinofuranosyl-2-fluoroadenine (fludarabine) can also substitute dATP to activate Apaf-1 (Leoni et al., 1998). On the other hand,

other nucleotides including CTP, dCTP, GTP, dGTP, TTP, and UTP are not able to support Apaf-1 function (Liu et al., 1996).

Apaf-1 Contains a dATP Cofactor.

Although ATP is much weaker in activating Apaf-1 than dATP, the cellular concentration of ATP is much higher than dATP. Therefore, it is unclear which nucleotide will be preferably used in vivo. Because the nucleotide-binding domain of Apaf-1 is closer to the N terminus than the WD-40 repeat region that may negatively regulate nucleotide binding, we hypothesized that Apaf-1 synthesized in cells might already contain a nucleotide cofactor. The identity of this bound nucleotide may give us a clue about which nucleotide is really used in cells.

The ability to make a large quantity of Apaf-1 recombinant protein in insect cells allowed us to directly examine this scenario. We first denatured purified Apaf-1 by phenol extraction, and then analyzed the aqueous phase in a liquid chromatography-mass spectrometry system (LC-MS). As shown in Fig. 2, a peak that matched the mass of dATP standard was observed when the small molecule associated with Apaf-1 was analyzed by LC-MS (Fig. 2 A and B). No ATP or dADP was observed under the same extraction and analysis condition, indicating that Apaf-1 indeed contains a dATP cofactor. The dATP

bound to Apaf-1 is stable because we did not see any dADP even after we incubated Apaf-1 alone *in vitro* for 3 h (data not shown).

Cytochrome *c* Induces dATP Hydrolysis.

Because Apaf-1 activity is triggered by cytochrome *c*, we checked the status of the dATP that bound to Apaf-1 after incubation with cytochrome *c*. As shown in Fig. 2C, we noticed the dATP peak completely disappeared after Apaf-1 was incubated with cytochrome *c* and a new peak correlated with dADP appeared. This finding suggested that cytochrome *c* induces hydrolysis of the Apaf-1-bound dATP to dADP.

To further analyze this hydrolysis event, we used a Malachite Green phosphate assay system that quantitatively measures the released phosphate after incubating purified Apaf-1 with cytochrome *c*. As shown in Fig. 3, there was no phosphate release when Apaf-1, or cytochrome *c* was incubated either alone or with dATP (pink and light blue lines and lines with filled red and dark blue circles). On the other hand, when Apaf-1 was incubated with cytochrome *c* (line with open red circle), the released phosphate was detected after 90-min incubation and the amount increased linearly up to 150 min. The released phosphate reached plateau around 30 pmol, close to the 35 pmol of Apaf-1 protein used in the reaction. Interestingly, the released phosphate remained

plateaued at this level even when 10 μ M exogenous dATP was added at the linear range of dATP hydrolysis, clearly indicating that dATP is hydrolyzed only once by Apaf-1 (line with open dark blue circle). The exogenously added dATP cannot be further hydrolyzed once one round of dATP hydrolysis is done.

Nucleotide Exchange on Apaf-1 During Apoptosome Formation.

How can we explain the requirement of exogenous dATP for apoptosome formation? The logical speculation is that there is a nucleotide exchange step after dATP hydrolysis. Without such an exchange step, Apaf-1 may fold into inactive configuration after the dATP hydrolysis. To further investigate this particular step, we analyzed apoptosome formation by using a glycerol gradient that can separate monomeric Apaf-1 from apoptosome. As shown in Fig. 4A, Apaf-1 alone migrated at fractions 3–4 on top of the gradient but shifted to fractions 6–8 after incubating with cytochrome *c* and dATP, the condition to form apoptosome. The functionality of apoptosome and Apaf-1 was confirmed by adding procaspase-9 and -3 and caspase-3 activity was measured (Fig. 4B). The free Apaf-1 at fractions 3–4 was active in activating caspase-3, and the preformed apoptosome peaked at fraction 7 (dark and light blue lines, respectively). In contrast, if Apaf-1 was preincubated with

cytochrome *c* in the absence of dATP, Apaf-1 protein formed aggregates that migrated to the bottom of the gradient (Fig. 4A Lower) and showed no caspase-3 activity even when procaspase-9 and -3 were added later (Fig. 4B, red line).

To confirm that there has to be a nucleotide exchange to form functional apoptosome, we added radioactive dATP to the apoptosome-forming reaction and isolated the apoptosome afterward by glycerol gradient. We then measured where the radioactive dATP went by liquid scintillation counting. As shown in Fig. 4C, the radioactive peak was correlated perfectly with that of apoptosome (peak at fraction 7). There was no radioactivity associated with monomeric Apaf-1 or aggregated Apaf-1, indicating that the nucleotide exchange only happens during apoptosome formation. To confirm the identity of the radioactive nucleotide associated with apoptosome, we formed and isolated apoptosome by using radio-labeled dATP. We then analyzed apoptosome-associated radioactivity with TLC. As shown in Fig. 4D, the radioactive nucleotide was confirmed by TLC as exclusively dATP.

Discussion

The above experiments revealed several previously unknown steps during apoptosome formation. As shown schematically in Fig. 5, Apaf-1 generated in insect cells contains dATP as a cofactor. The bound dATP then undergoes one round of hydrolysis to dADP, a process that is stimulated by cytochrome *c*. This hydrolysis appears to serve two roles: (i) it provides energy for the conformational change need for Apaf-1 to transient from the inactive monomeric state to the oligomeric state; and (ii) it allows exogenous dATP (or ATP) to exchange for the dADP that has lower binding affinity for Apaf-1, a critical step for Apaf-1 to form functional apoptosome rather than nonfunctional aggregates. This hydrolysis only happens in one round. Exogenously added dATP will then bind Apaf-1, but remains unhydrolyzed during apoptosome formation.

The formation of the nonfunctional Apaf-1 aggregate is also induced by cytochrome *c* binding to Apaf-1. We actually reisolated cytochrome *c* as an inhibitor of Apaf-1 activity when dATP or ATP was not included in the caspase-3-activating reaction (M.F. and X.W., data not shown). Such aggregates may be identical to the large, inactive Apaf-1 complex first observed in human monocytic tumor cells (Cain et al., 2000).

Interestingly, the crystal structure of a WD-40-truncated Apaf-1 revealed Apaf-1 in an inactive configuration with an ADP bound to it (Riedl et

al., 2005). Because WD-40 repeats serve as an autoinhibitory role, Apaf-1 without this region should be active, yet may easily become inactive if the exogenous dATP or ATP level is low. This finding is consistent with previous observation that WD-40-less Apaf-1 is indeed active in promoting procaspase-9/3 activation but is rather unstable and the only stable configuration might be the dADP or ADP binding form (Srinivasula et al., 1998; Adrain et al., 1999; Riedl et al., 2005). It is also interesting that this form of Apaf-1 expressed in bacteria contains an ADP but not dADP, whereas full-length Apaf-1 expressed in insect cells contains exclusively dATP. The measured difference between dATP and ATP in binding affinity to Apaf-1 is 10-fold, not enough to explain this exclusive binding of dATP because intracellular ATP level is several orders of magnitude higher than dATP (Jiang and Wang, 2000). One possibility is that dATP level in *E. coli* is very low. Another possibility could be that mammalian and insect cells contain a dATP-specific loading factor for Apaf-1 that is absent in bacteria. Such a factor could potentially function in conjunction with prothymosin- α and PHAPI, two proteins that regulate apoptosome activity (Jiang et al., 2003).

The role of cytochrome *c* in apoptosome formation also becomes clear through the current study. Upon binding to Apaf-1, cytochrome *c* releases the

autoinhibition imposed by the WD-40 repeats and allows Apaf-1 to hydrolyze the bound dATP.

This role of cytochrome *c* also suggests that its simple release from mitochondria and binding to Apaf-1 may not necessarily result in the activation of caspase-9/3. Without exogenous dATP or ATP exchange, cytochrome *c* binding to Apaf-1 will irreversibly deplete the Apaf-1 protein in cells without activating caspases. Consistently, when intracellular ATP is depleted, cells undergo necrosis in response to stimuli that normally induce apoptosis, and when the cellular ATP levels are restored, the response shifts back to apoptosis (Eguchi, Shimizu and Tsujimoto, 1997). Therefore, we hypothesize that the nucleotide exchange on Apaf-1 may provide another regulatory step for apoptosis.

The question remains whether endogenous Apaf-1 in mammalian cells also exclusively binds dATP. Addressing this question requires improvement on LC-MS method so that we can identify the nucleotide bound to endogenous Apaf-1 by using much less available material.

Experimental Procedures

Materials

Nucleotides dATP and dADP were purchased from Amersham Pharmacia; [α -³³P]dATP was obtained from MP Bioscience. Polyclonal antibodies against Apaf-1, Caspase-9, and Caspase-3 were prepared as described (Jiang and Wang, 2000).

Production of Proteins

Purified horse cytochrome *c* was prepared as described (Liu et al., 1996) followed by Mono S chromatography using the SMART system (Amersham Pharmacia). Apaf-1 cDNA was amplified with oligonucleotides 5'-AGTCGCGGCCGCATGCACCACCATCATCACCACATGGATGCA A A AGCTCGAAATTGTTTGC-3' and 5'-CTTCTCGACAAGCTTGGTACCTTAATGATG-3', using full-length Apaf-1 pFastBacI construct (Zou et al., 1999) as template. A 3.8-kb PCR product was ligated into the pGEM-T Easy vector by using the TA cloning kit (Promega). Plasmid was sequenced and mutations were corrected by using a QuikChange Site-Directed Mutagenesis kit (Stratagene). Corrected Apaf-1 cDNA with six N-terminal histidines and nine C-terminal histidines was then subcloned into NotI/KpnI sites of pFastBacI (Invitrogen). The pFASTBACI containing the correct Apaf-1 cDNA was then used to make baculovirus, and the recombinant Apaf-1 protein was produced in SF21 cells after infection with the baculovirus

according to the manufacturer's instruction. All of the plasmid manipulation and amplification for Apaf-1 were done at <16°C to prevent recombination.

Recombinant Apaf-1 was then expressed and nickel affinity-purified as described (Zou et al., 1999), followed by Hitrap Q, Heparin, and Superdex 200 chromatography using a fast protein liquid chromatography system (Amersham Pharmacia). Recombinant procaspase-9 and procaspase-3 were expressed and purified as described (Jiang and Wang, 2000), followed by a Hitrap Q column purification.

Detection of Apaf-1 Bound Nucleotides by LC-MS

Measurement of dATP Hydrolysis by Apaf-1. The Malachite Green Phosphate Assay kit (POMG-25H, BioAssay Systems) was purchased for measuring dATP hydrolysis. The reaction was carried out in buffer A (20 mM Hepes-KOH, pH 7.5/10 mM KCl/1.5 mM MgCl₂/1 mM EDTA/1 mM EGTA/1 mM DTT/0.1 mM PMSF) containing an additional 5 mM MgCl₂, 35 pmol of Apaf-1, 175 pmol of cytochrome *c*, and other factors as indicated in Fig. 3. Hydrolysis of dATP was measured in a XFluor4 spectrometry reader (Tecan) as instructed in the manual (BioAssay Systems)

Glycerol Gradient and Measurement of Apoptosome Activity. Twenty nanograms of purified Apaf-1 and other components indicated in Fig. 4 were incubated at 30°C for 3 h. Samples were then applied onto a 10–30% glycerol

gradient in 3.6 ml and centrifuged at 50,000 rpm (256,000 x g) at 17°C for 3 h, using SW60Ti rotor (Beckman). Fractions were taken from the top of tube by using a pipette (15 fractions, 240 µl per fraction). Fractions were then used for the Western blotting for Apaf-1 and other assays below.

Apoptosome activity was measured by incubating a 14-µl aliquot of each fraction with 50 nM procaspase-9, 50 nM procaspase-3, 10 µM dATP, 100 nM cytochrome *c*, and 10 µM fluorogenic DEVD caspase-3 substrate. Samples were transferred to 384-well microplate, and caspase-3 activity was measured by using XFluor4 spectrometry reader (Tecan) (Cain et al., 2000).

TLC

PEI Cellulose TLC plate was purchased from Selecto Scientific (Suwanee, GA). Active and inactive apoptosome samples were fractionated by Superose 6 chromatography using a SMART system as described (Jiang and Wang ,2000). A 3-µl aliquot of Apaf-1 peak fraction from each sample was spotted on to the TLC plate and separated in the separation buffer (1 M formic acid/0.5 M LiCl). The TLC plate was dried and exposed to BAS-III plate (Fuji) and visualized by Typhoon PhosphorImager and IMAGEQUANT software (Molecular Dynamics).

Apaf-1 bound nucleotides were analyzed by using a liquid chromatographymass spectrometry system (LC-MS, Shimazu). All of the

samples were dialyzed at 4°C for 2 h to remove salt and extra nucleotides after incubation of Apaf-1 in the absence or presence of cytochrome *c*. Nucleotides were extracted in the aqueous phase by using phenol/chloroform/isoamyl alcohol (25:24:1, vol/vol, Roche). Samples were then dialyzed against distilled water for 4 h by using dialysis tube with a cutoff molecular mass of 500 Da (Spectrum). The samples were then applied to LC-MS by using ESI polarity switching with column method (1–70% of MeOH/H₂O gradient).

Figure 1.

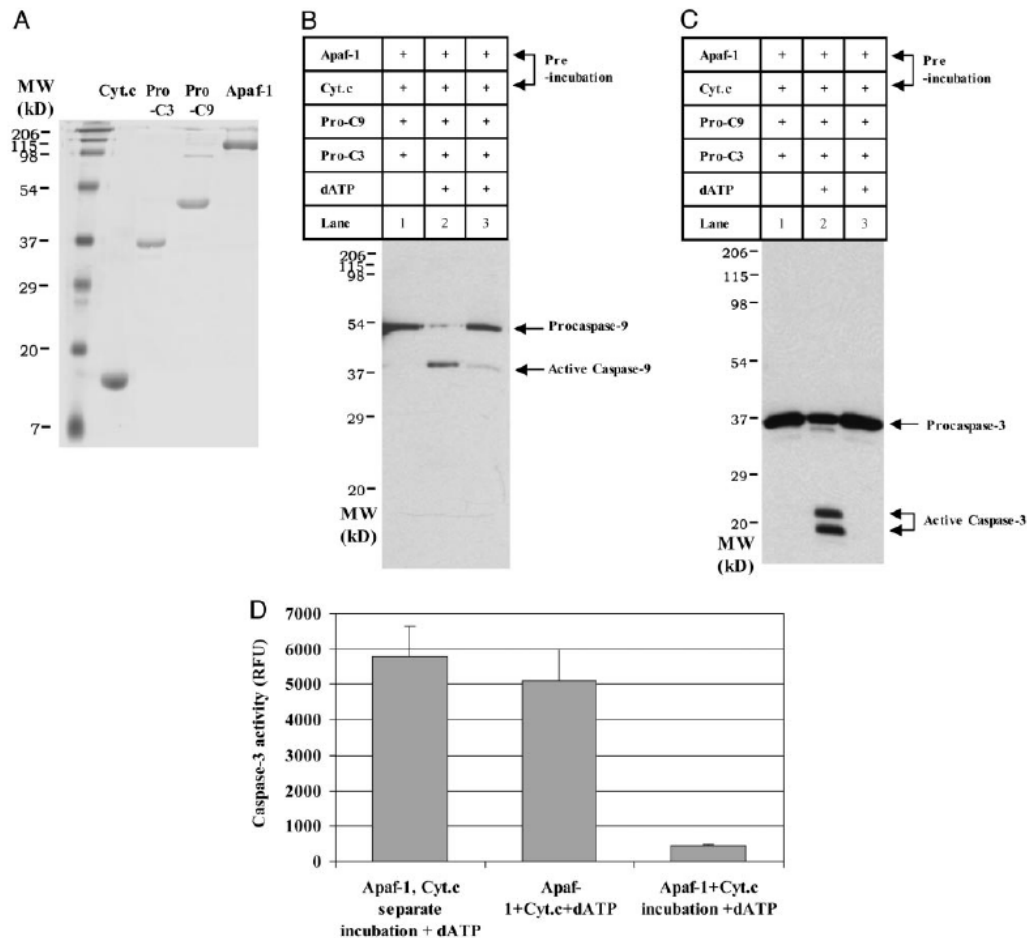


Fig. 3-1. Apaf-1-mediated caspase activation. (A) Coomassie blue staining of purified horse heart cytochrome *c* (Cyt.c) and recombinant Apaf-1, pro-caspase-9 (Pro-C9), and pro-caspase-3 (Pro-C3) (1 μ g of protein each). (B and C) Western blot of caspase-9 and caspase-3, respectively. Apaf-1 at a final concentration of 20 nM was incubated with cytochrome *c* (Cyt.c, 100 nM final concentration), procaspase-9 (Pro-C9), and procaspase-3 (Pro-C3) at a final concentration of 50 nM in the absence or presence of 10 μ M dATP at 30°C for 1.5 h in a final volume of 20 μ l (lanes 1 and 2). In lane 3, Apaf-1 and cytochrome *c* were preincubated at 30°C for 1 h before the addition of procaspase-9, procaspase-3, and dATP and incubated at 30°C for 1.5 h. The samples were subsequently subjected to SDS/PAGE followed by Western blotting analysis using antibodies against caspase-9 and caspase-3. Cleaved products of procaspase-9 and procaspase-3 are labeled as active caspases. (D) The graph shows the caspase-3 activity measured by fluorogenic caspase-3 substrate. Apaf-1 (20 nM) and cytochrome *c* (100 nM) were preincubated separately at 30°C for 1 h, then incubated with

other components (50 nM procaspase-9, 50 nM procaspase-3, and 10 μ M dATP) at 30°C for 1 h in a final volume of 20 μ l(Left). Apaf-1 and cytochrome *c* were incubated together with other components at 30°C for 1 h (Center). Apaf-1 and cytochrome *c* were preincubated together at 30°C for 1 h, then incubated with dATP and other components at 30°C for 1 h (Right). Fluorogenic caspase-3 substrate was added to each sample after the incubation to measure the substrate cleavage as described in Materials and Methods.

Figure 2.

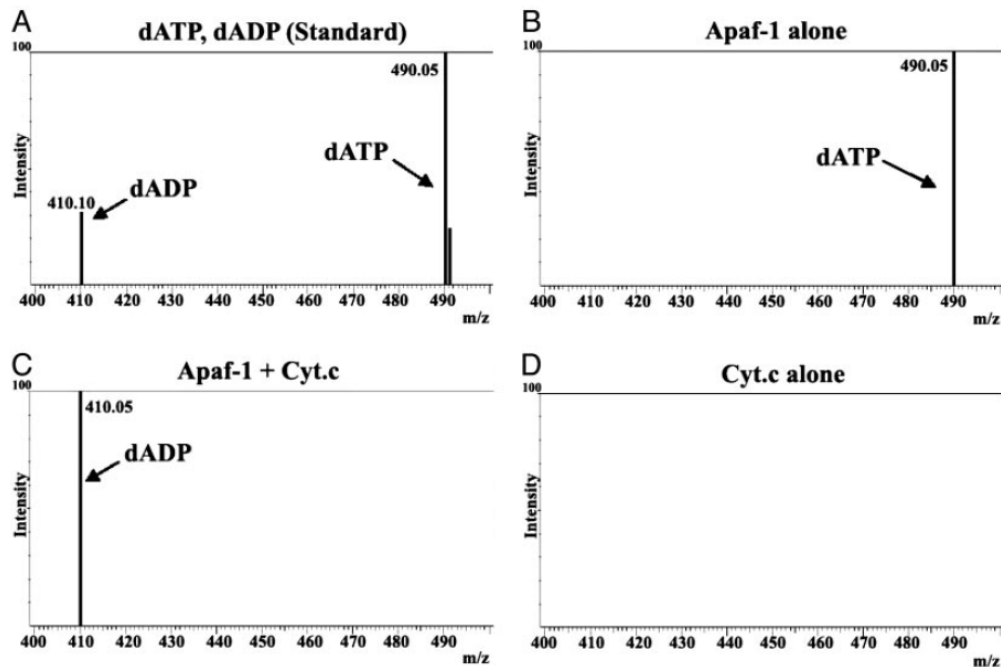


Fig. 3-2. Apaf-1 is associated with dATP and hydrolyzes it upon cytochrome *c* binding. (A) A mixture of dATP and dADP analyzed by LC-MS. (B) LC-MS analysis of aqueous phase after 40 ng of recombinant Apaf-1 protein was extracted with phenol as described in Materials and Methods. A mass peak correlated with dATP was indicated. (C) LC-MS analysis was done as in B, but 40 ng of recombinant Apaf-1 was incubated with 20 ng of cytochrome *c* for 3 h before extraction with phenol. A mass peak correlated with dADP was indicated. (D) LC-MS analysis of aqueous phase after cytochrome *c* alone was extracted with phenol.

Figure 3.

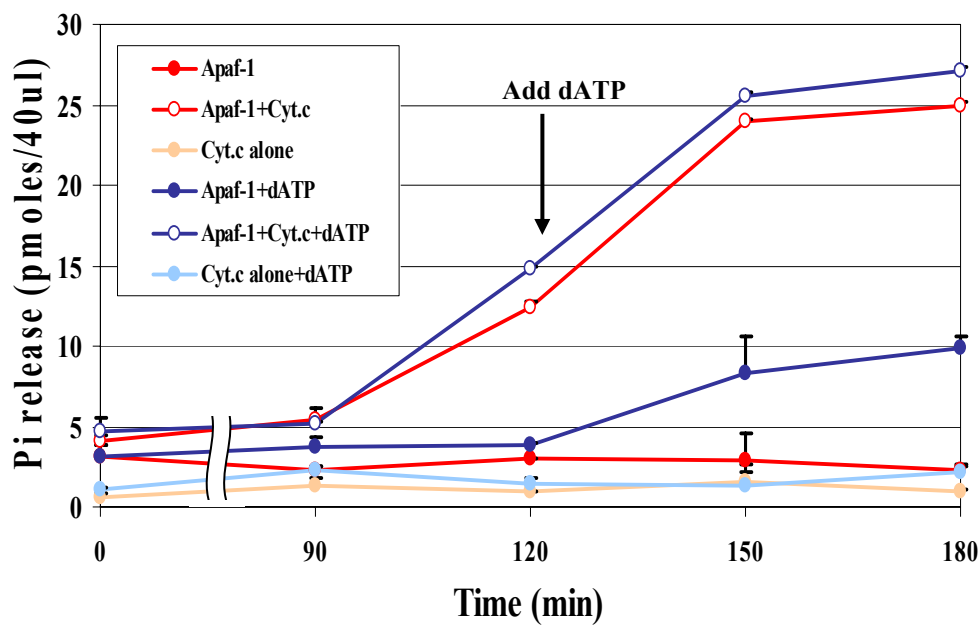


Fig. 3-3. Cytochrome *c*-stimulated dATP hydrolysis by Apaf-1. Apaf-1 (35 pmol) and cytochrome *c* (175 pmol) were used in a final volume of 40 μ l. Aliquots of Apaf-1 alone (filled red circle), Apaf-1 plus cytochrome *c* (open red circle), and cytochrome *c* alone (filled pink circle) were incubated at 30°C for 3 h, and dATP hydrolysis was measured at the indicated time points as described in Materials and Methods. For the other three samples, 10 μ M of dATP was added to Apaf-1 alone (filled dark blue circle), Apaf-1 plus cytochrome *c* (open dark blue circle), or cytochrome *c* alone (filled light blue circle) 2 h after the starting incubation. The dATP hydrolysis was measured by a Malachite Green Phosphate Assay kit as described in Materials and Methods.

Figure 4.

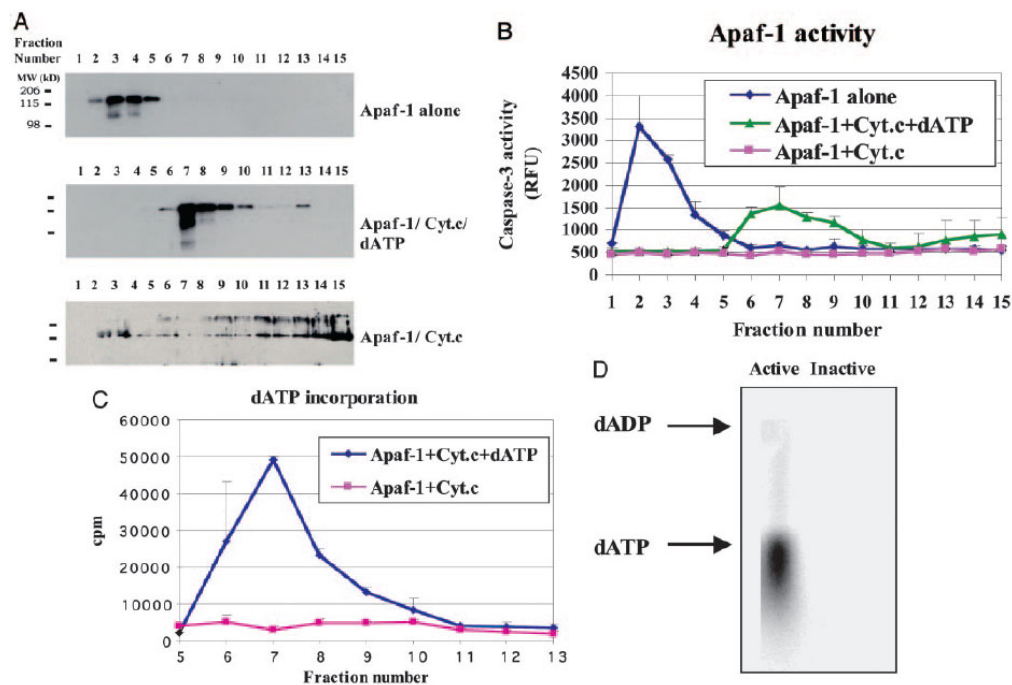


Fig. 3-4. Apoptosome contains exogenously added dATP. (A) Indicated samples were subjected to glycerol gradient separation after incubation as described in Materials and Methods. Fractions from the glycerol gradient were subjected to SDS/PAGE followed by Western blotting using anti-Apaf-1 antibody. (B) The same glycerol gradient fractions as in A were subjected to caspase-3 activity assay. Aliquots (14 μ l) of glycerol gradient fractions were incubated with 50 nM procaspase-9, 50 nM procaspase-3, 10 μ M dATP, 100 nM cytochrome *c*, and 10 μ M fluorogenic DEVD caspase substrate in a final volume of 20 μ l. Samples were mixed in the test tubes and transferred to 384-well microplates, and caspase-3 activity was measured by using the XFluor4 spectrometry reader (Tecan). (C) dATP incorporation was measured by using [33 P]dATP. A total of 10 μ Ci of [33 P]dATP plus 10 μ M of dATP were incubated with Apaf-1 and cytochrome *c* at 30°C for 3 h (blue diamond). For another sample, 10 μ Ci of [33 P] dATP plus 10 μ M of dATP was added to Apaf-1 and cytochrome *c* mixture after they were preincubated for 1.5 h. The sample was incubated for additional 1.5 h before being subjected to glycerol gradient (pink square). The fractions were then collected as in A, and a 4- μ l aliquot of each fraction was counted for radioactivity by a liquid scintillation counter. (D) For the active apoptosome, 10 ng of Apaf-1, 5 ng of cytochrome *c*, and 10 μ Ci of [33 P]dATP plus 10 μ M of dATP were incubated at 30°C for 3 h before being subjected to a Superpose 6 chromatography column as described in Materials and Methods. For the inactive apoptosome sample, 10 ng of Apaf-1 and 5 ng of cytochrome *c* were preincubated at 30°C for 1.5 h. Then, 10 μ Ci of [33 P]dATP plus 10 μ M of dATP were added to the sample, and incubation was continued for 1.5 h before the sample was subjected to the Superpose 6 gel-filtration column. An aliquot of 3 μ l of peak Apaf-1 fraction was spotted on a TLC plate and analyzed as described in Materials and Methods.

Figure 5.

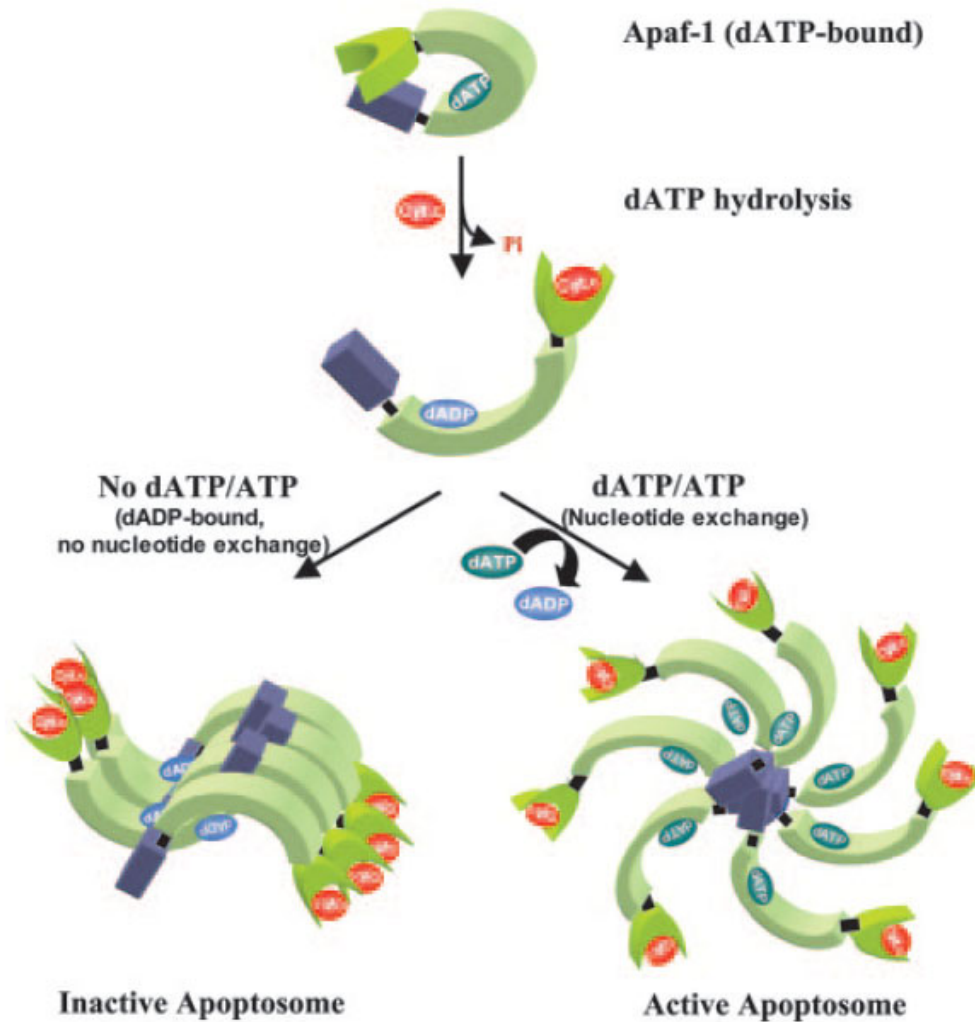


Fig. 3-5. Model of apoptosome formation. Apaf-1 is associated with dATP. Upon cytochrome *c* binding, Apaf-1 hydrolyzes dATP. If there is extra dATP/ATP, dADP is exchanged with dATP and Apaf-1 forms the active apoptosome. When Apaf-1 is incubated with cytochrome *c* without extra dATP/ATP, dADP-bound Apaf-1 forms the inactive aggregate.

Chapter 4 : CAS Is a Mediator of PHAPI and Positively Regulates Apoptosome by Enhancing Nucleotide Exchange on Apaf-1

Abstract

Apaf-1 undergoes conformational changes to assemble the apoptosome when cytochrome *c* binds to it. Apoptosome formation process includes several biochemical steps to carry out successful Apaf-1 assembly, such as dATP hydrolysis and dATP/ATP exchange on Apaf-1. Cytochrome *c* binding initiates the first dATP hydrolysis on Apaf-1 then; the hydrolyzed nucleotide is exchanged with dATP/ATP to form an active apoptosome. PHAPI positively regulates apoptosome formation by increasing caspase-9 activation. However, the detailed mechanism of PHAPI function on apoptosome is remained to be determined. Biochemical fractionation of cell extracts led us to identify a cellular apoptosis susceptibility protein (CAS) as a mediator of PHAPI. CAS is a multifunctional protein involved in various cellular processes including proliferation and apoptosis. CAS, together with PHAPI, enhances nucleotide exchange on Apaf-1 during apoptosome formation. Thus, it facilitates apoptosome formation upon apoptotic stimuli.

Introduction

Apoptosis is a specific form of cell death operating as a cellular suicidal program. The characteristic apoptotic markers such as nuclear condensation, nuclei fragmentation, DNA fragmentation, membrane blebbing, and breakdown of cells into small apoptotic bodies are executed by activation of caspases (Wyllie, 1980a; Wyllie, 1980b). Caspases are cysteine proteases that cleave their substrates after aspartate residues. Caspases are activated by proteolytic cleavage as a result of a cascade of biochemical reactions (Thornberry, 1998).

The signaling pathways to activate caspases are categorized into the extrinsic or intrinsic apoptotic pathways. The extrinsic pathway is triggered by extracellular ligands, which bind to cell surface receptors. Cytosolic adaptor proteins are recruited to the receptor to form a complex and activate initiator caspases such as procaspase-8. As a result, downstream effector caspases are activated to promote apoptosis (Nagata, 1999). The intrinsic pathway is initiated from the mitochondria. Apoptotic stimuli triggers release of cytochrome *c* from the mitochondria to initiate caspase activation (Liu et al., 1996; Zou, 1997). Cytochrome *c* binds to WD-40 repeats region on Apaf-1 and induces conformational change in Apaf-1. Upon cytochrome *c* binding, Apaf-1 gets activated and hydrolyzes its bound nucleotide most likely to provide

energy for conformational change. Then, seven molecules of Apaf-1 oligomerize and form an active apoptosome in the presence of nucleotides dATP or ATP that would replace hydrolyzed nucleotides (Kim et al., 2005). The apoptosome serves as a platform to recruit and activate an initiator caspase, procaspase-9, via interaction between CARD domains on Apaf-1 and procaspase-9. Caspase-9-loaded apoptosome then cleaves the downstream effector caspases such as caspase-3 and caspase-7, whose activation leads to apoptosis through substrates cleavage (Li et al., 1997).

Apaf-1 activity can be regulated by controlling cytosolic release of cytochrome *c* to inhibit or promote apoptosome formation. Cytochrome *c* release upon apoptotic stimuli is regulated by Bcl-2 family of proteins (Gross et al., 1999; Martinou, 2001). Anti-apoptotic members of Bcl-2 family proteins such as Bcl-2, Bcl-xL and Mcl-1 can inhibit apoptosome formation by protecting mitochondrial integrity. On the other hand, pro-apoptotic members of Bcl-2 family proteins can induce apoptosome formation by releasing cytochrome *c*, and at the same time promoting caspase activation downstream of apoptosome formation by releasing apoptogenic factors such as Smac.

Also, the cellular ATP level is one of the factors that regulate apoptosis. Under intracellular ATP-depleting conditions, cells undergo necrosis upon apoptotic stimuli, which would otherwise trigger apoptosis when intracellular

ATP level is restored (Eguchi et al., 1997). Consistently, cellular ATP depletion blocks caspase-9 activation in response to apoptotic stimuli while cytochrome *c* release is not affected (Eguchi et al., 1999). This observation supports the idea that apoptosome activity is regulated by intracellular level of nucleotides.

Previously, we identified a novel pathway that both positively and negatively regulates Apaf-1 protein at a distinctive level (Jiang et al., 2003). This pathway consists of PHAP proteins as positive regulators and prothymosin- α as a negative regulator for mitochondria-initiated caspase activation. PHAP proteins promote caspase-9 activation possibly by facilitating active apoptosome formation or recruiting more caspase-9 to the apoptosome. Prothymosin- α inhibits caspase-9 activation by negatively regulating apoptosome formation. It is clear these regulators affect Apaf-1 function to regulate caspase activation; however, the detailed biochemical mechanism is still unclear. As nucleotide hydrolysis and exchange plays an important role on Apaf-1 oligomerization, it becomes a critical question whether this novel pathway affects apoptosome assembly by regulating at nucleotide hydrolysis or exchange steps. To further understand how PHAP proteins regulate the apoptosome, we established a cell-free *in vitro* assay for finding out additional players in this pathway. Biochemical fractionation of HeLa cell extract led us

to identify CAS (cellular apoptosis susceptibility protein) as a mediator of PHAP proteins. Here we show biochemical analysis of this novel caspase-activating pathway demonstrating the mechanism by which PHAPI and CAS have stimulates apoptosome-dependent caspase activation.

Results and Discussion

***In vitro* reconstitution of PHAPI pathway**

PHAP family of proteins stimulates apoptosome activity by an undefined mechanism. Previously, we showed that PHAPI protein activates more caspase-9 by increasing the recruitment of procaspase-9 to apoptosome using a partially purified system (Jiang et al., 2003). When we tried a purified system using recombinant proteins, we failed to reconstitute the apoptosome regulation *in vitro*, suggesting that there are more players involved in this novel pathway. To study how PHAP proteins positively regulate apoptosome function, we set up an *in vitro* assay to identify its mediator. The assay measures apoptosome activity *in vitro* by measuring the caspase-3 activity, using endogenously purified Apaf-1 and recombinant proteins for the other components. Figure 1A shows the purified proteins we used for the assay using coomassie blue staining. The potential PHAPI mediator can be separated from

other known factors that positively regulate apoptosome, such as caspases, and cytochrome *c* by Q-sepharose anion exchange column (data not shown). On the other hand, we failed to separate the potential mediator from Apaf-1. The mediator co-migrated with Apaf-1 on most of the columns we tried. However, we were able to separate the potential PHAPI mediator from Apaf-1 By precipitating Apaf-1 and the mediator containing fractions from Q-sepharose column with 40% ammonium sulfate. In Figure 1B, mixture of endogenous Apaf-1, procaspase-9, cytochrome *c*, dATP and PHAPI did not activate caspase-3. When we co-incubate the resuspended pellet from 40% ammonium sulfate precipitates described above (P, see the Experimental Procedures for detail) with PHAPI and the other components, we were able to see caspase-3 activation. This indicated that the potential mediator of PHAPI was in that fraction. We used this material as a starting material to purify the PHAPI mediator.

However, we had trouble to purify this protein to homogeneity using the conventional biochemical fractionation method. This mediator migrated with Apaf-1 in different columns suggesting that it may physically interact with Apaf-1. Thus, we attempted to use protein-protein interaction to help our purification. We incubated six N-terminal histidines and nine C-terminal histidine tagged recombinant Apaf-1 with S-100 from Apaf-1 knockout MEF

cells at 4 °C. Then, we re-purified the recombinant Apaf-1 using nickel affinity beads and used the recovered Apaf-1 for the assay. The re-purified recombinant Apaf-1 from Apaf-1-null S-100 was able to respond to PHAPI and activate caspase-3 (Figure 1C). This suggested that the recombinant Apaf-1 interacted with the potential PHAPI mediator in Apaf-1-null S-100.

Identification of CAS as a mediator of PHAPI

Using the properties of the mediator protein described above, we performed protein fractionation using HeLa cell S-100 as shown in Figure 2A. First, we applied HeLa cell S-100 to Q sepharose column to get Apaf-1 containing fractions that also include the potential PHAPI mediator. Then, we pooled the fractions and precipitated it with 40% of ammonium sulfate. This step allowed the mediator to dissociate from Apaf-1. The pelleted precipitates were resuspended and loaded onto a superdex 200 gel filtration column. The stimulatory activity for caspase-3 in the presence of PHAPI was collected and loaded onto a Heparin column. The activity did not bind to the column and flew-through Heparin column. However, after incubation with recombinant Apaf-1, the activity was no longer in Heparin flow-through. The Heparin fractions were stained by silver staining as shown in Figure 2B.

Three protein bands that co-migrated with recombinant Apaf-1 on Heparin column were identified as cellular apoptosis susceptibility protein (CAS). CAS was cloned as an apoptosis susceptibility gene, as the antisense cDNA fragments of CAS made MCF-7 cells resistant to both toxin and tumor necrosis factor (TNF) induced cell death (Brinkmann et al., 1995). CAS is located in chromosome 20q13, a locus amplified in various cancer cells including colon cancer and breast cancer. Also, CAS is thought to be involved in multiple cellular processes, such as cell proliferation, nuclear export of importin α , and taxol-induced apoptosis in several cancer cells *in vitro* (Behrens et al., 2003). To confirm we identified the right protein as a mediator of PHAPI, we then made recombinant CAS and checked its ability to activate caspase-3 (Figure 3A). Recombinant CAS was able to stimulate purified endogenous Apaf-1 to activate caspase-3 when PHAPI was added to assay mixture.

When we fractionated HeLa S-100 on Hitrap-Q column and took the Apaf-1 fractions, the partially purified Apaf-1 fractions activated caspase-9 and caspase-3 in the presence of PHAPI. We reasoned that it is because the partially purified Apaf-1 is associated with CAS. Then we tested if partially purified Apaf-1 would still be able to activate caspase-3 when we knock down endogenous CAS in cells. We knocked down the protein expression of

endogenous CAS in HeLa cells using siRNA transfection, and then took the Apaf-1 containing fractions from Hitrap Q-column. The Apaf-1 fraction from the CAS knock down cells failed to activate caspase-3 in the presence of PHAPI while the Apaf-1 fraction from control RNAi cells still had ability to activate caspase-3 when PHAPI was added. We were able to see caspase-3 activation using Apaf-1 fraction from CAS knock down cells, only when PHAPI was added together with recombinant CAS (Figure 3B).

However, we still could not replace purified endogenous Apaf-1 with recombinant Apaf-1 in our *in vitro* assay, implying that there still are missing factor(s), which is critical for PHAPI and CAS to regulate apoptosome.

Total *in vitro* reconstitution with recombinant proteins

As we could use re-purified recombinant Apaf-1 from Apaf-1-null S-100 for *in vitro* assay (Figure 1C), we had a clue that the missing factor might be another Apaf-1 associated protein. Since only endogenous Apaf-1 responded to PHAPI and CAS, and the endogenous Apaf-1 was purified close to homogeneity, the missing factor must be tightly associated with Apaf-1. To identify the missing factor, we looked for Apaf-1-associated proteins. Previously we had identified Hsp70 as an Apaf-1-associated protein by stringent pull-down experiment (Feng M and Wang X, unpublished result).

Therefore, we decided to check if Hsp70 was still associated with purified endogenous Apaf-1 and if so, check if PHAPI/CAS mediated apoptosome stimulatory activity could be reconstituted *in vitro* by adding Hsp70 to the assay mixture.

Hsp70 was detected by western blotting from purified endogenous Apaf-1 even after several steps of column purification (Figure 4A), while recombinant Apaf-1 did not contain any associated Hsp70. Roughly about 10 nM of Hsp70 was associated with 30 nM of purified endogenous Apaf-1. Then, we tested the Hsp70 protein in our *in vitro* assay (Figure 4B). Indeed, we were able to see caspase-3 activation with addition of CAS using recombinant Hsp70 and recombinant Apaf-1 with other components. More interestingly, we were able to demonstrate the negative effect of prothymosin- α on apoptosome using fully reconstituted system (Figure 4C and D). Adding PHAPI and CAS stimulated caspase-3 activation while addition of Prothymosin- α inhibited it. Also, when we added the small molecule PETCM on top of PHAPI, CAS and Prothymosin- α , we were able to remove the inhibition of Prothymosin- α and activate caspase-3. Interestingly, the functional dead mutant of Hsp70 (Hsp70AAAA) (Beere et al., 2000; Freeman et al., 1995) lost the ability to reconstitute apoptosome regulatory pathways. Hsp70AAAA has defects in substrate binding and has an enhanced ATPase activity.

PHAPI and CAS help dATP exchange

Taking advantage of the total *in vitro* reconstitution system, we wanted to study how PHAPI and CAS stimulate caspase-3 activation. In a previous study, we found that PHAPI could stimulate more caspase-9 activation (Jiang et al., 2003). It may be due to more procaspase-9 loading to apoptosome, or PHAPI may stimulate more active apoptosome formation that is preferable for procaspase-9 loading. In the process of apoptosome formation, Apaf-1 undergoes dynamic conformational changes, which require cytochrome *c* binding and nucleotide hydrolysis and exchange. Apaf-1 hydrolyzes its bound nucleotide upon cytochrome *c* binding. To form active apoptosome, hydrolyzed nucleotide needs to be exchanged. The nucleotide exchange can be carried out in the absence of exchange factor or nucleotide loading factor *in vitro*, when high concentration of Apaf-1 is used (Kim et al., 2005). Yet, when used in low concentration (15 nM) similar to endogenous level, Apaf-1 failed to activate downstream caspases even though cytochrome *c* and dATP were supplied (Figure 4C). Therefore, we hypothesized that PHAPI and CAS may function on the nucleotide exchange step to stimulate apoptosome formation. To test this hypothesis, we checked nucleotide loading with or without PHAPI and CAS (Figure 5A).

We incubated recombinant Apaf-1 and Hsp70 with cytochrome *c* and dATP in the condition that does not stimulate caspase activation. Radiolabeled dATP would be loaded onto Apaf-1 in exchange with hydrolyzed nucleotides. After incubation as indicated in Figure 5, we used TLC plate to measure how much radiolabeled dATP was loaded onto Apaf-1. Consistent with the caspase-3 activity assay (Figure 4C), only minor incorporation of dATP was detected at 90 minutes and 120 minutes after incubation (Figure 5A, Lane 1-5). On the other hand, as we hypothesized, PHAPI and CAS significantly increased dATP loading onto Apaf-1 (Figure 5A, Lane 6-10). dATP loading was saturated after 90 minutes. The arbitrary unit of volume quantification is shown at the right panel. Since we can consider Apaf-1 as an ATPase enzyme and dATP as its substrate, we calculated K_s for Apaf-1 and dATP complex (Figure 5B). We measured Apaf-1-dATP complex formation by the filter binding experiment after indicated incubation. Adding PHAPI and CAS increased dATP loading to Apaf-1 more than one thousand folds, and slightly increased K_s compared to Apaf-1 without PHAPI and CAS. Consistently, apoptosome formation was indeed facilitated and caspase-9 activation was accelerated when PHAPI and CAS were incubated together with Apaf-1 in the mixture (Figure 5C). When Apaf-1 was incubated with cytochrome *c* and dATP in the presence of Hsp70, the small portion of Apaf-1 spreaded throughout the gel filtration column. It

may be representing the inefficient Apaf-1 assembly due to lack of nucleotide exchange. It is consistent with our previous observation that Apaf-1 tends to aggregate in the absence of nucleotide exchange (Kim et al., 2005). When PHAPI and CAS were added, more apoptosome was formed. This apoptosome were able to activate caspase-9 efficiently.

Based on these results, we suggest that PHAPI and CAS stimulate apoptosome formation by accelerating Apaf-1's nucleotide exchange at downstream of cytochrome *c* binding.

***In vivo* knock down of CAS**

To test if CAS has *in vivo* relevance to cellular apoptosis, we made tetracycline-inducible shRNA expressing CAS knock-down cell line using HT-29 colon cancer cells. We were not able to make CAS knock-down stable cell line using HeLa cells as CAS knock-down interfered with mitosis in HeLa cells. HT-29 cells express relatively low amount of CAS and CAS expression is induced under cell death stress such as Interferon- γ or UV. CAS overexpression in HT-29 cells did not induced apoptosis, yet CAS overexpression enhanced apoptosis in Interferon- γ treated HT-29 cells, indicating CAS plays a role in apoptosis (Jiang et al., 2001). Therefore, HT-29

cells were suitable to carry out our purpose since low expression of CAS was sufficient to maintain cell cycle in this cell line.

We selected 3 clones that induced shRNA expression upon tetracycline treatment. These clones successfully knocked down CAS expression after 72 hours of tetracycline treatment (Figure 6A). Cell survival was measured after lethal dose of UV treatment. HT-29 cells were sensitive to UV treatment. However, when CAS was knock down, the cells became resistant to UV-induced apoptosis (Figure 6B). All three clones presented similar cell death profiles upon UV treatment in the absence or presence of tetracycline (Figure 6B). To exclude off-target effect of shRNA induced knock down, we expressed RNAi resistant full-length CAS. The target sequence of shRNA in CAS gene was scrambled without changing amino acid codons (Figure 6A). The scrambled CAS construct was transiently transfected to each clone (Figure 6A and C). Endogenous CAS protein disappeared after tetracycline treatment; while exogenously transfected scrambled CAS expression was not affected by tetracycline (Figure 6A). Scrambled CAS migrated slower in gel because it has higher molecular weight with three repeats of FLAG peptides tag at its C-terminus. CAS knock down cells were still resistant to UV treatment. Furthermore, exogenous scrambled CAS expression rescued cell death phenotype and sensitized cells to UV treatment in all three clones (Figure 6C).

In summary, we identified CAS as a mediator of PHAPI and Hsp70 as a critical player in this novel pathway. CAS is a multifunctional protein involved in various cellular processes including apoptosis. Its one of many functions in apoptosis may be regulating apoptosome formation as we presented in this article. PHAPI and CAS act together to accelerate nucleotide exchange on Apaf-1 to facilitate apoptosome formation. We do not know the clear function of Hsp70 in this pathway; nonetheless Hsp70 was required to deliver the regulatory effect of PHAPI and CAS on Apaf-1. Hsp70 mutant, whose C-terminal 4 amino acid residues were changed to 4 alanines, failed to carry out its function on Apaf-1. Hsp70 may be a key chaperon protein when Apaf-1 undergoes conformational changes. Lastly, we showed that CAS has cell death regulatory function *in vivo* using inducible knock down and rescue experiments.

Identification of PHAPI mediator and reconstitution of the novel apoptosome regulatory pathway with highly purified recombinant proteins described in this article revealed the previously unknown properties of apoptosome. With the concentration of Apaf-1 that is close to the level of endogenous Apaf-1 (15~20 nM), and 10 μ M of dATP was not sufficient to promote caspase-3 activation. However, when PHAPI and CAS were present,

Apaf-1 was able to activate caspase-3 effectively. We biochemically purified CAS protein as a mediator of PHAPI. We also showed that PHAPI and CAS accelerated nucleotide exchange during apoptosome formation and stimulated to form an active apoptosome, which was able to activate downstream caspases successfully.

PHAPI does not seem to be associated with apoptosome (Hill, 2004). If there is any interaction between Apaf-1 and PHAPI, that must be very weak to detect. Meanwhile, CAS was associated with Apaf-1 and promoted apoptosome formation when PHAPI was present. Neither CAS nor PHAPI alone were able to affect apoptosome formation (data not shown). Only when CAS and PHAPI were incubated together, we were able to see the positive effect. However, how CAS and PHAPI work cooperatively to facilitate nucleotide exchange in Apaf-1 is still not clear. Which domain of Apaf-1 interacts with CAS and PHAPI needs to be determined to understand the mechanism how CAS regulate apoptosome. Whether PHAPI and CAS accelerate nucleotide exchange by increasing initial nucleotide hydrolysis is not clear at this point. We encountered technical difficulty to measure initial nucleotide hydrolysis using physiological concentration of recombinant proteins.

CAS is a multifunctional protein involved in both cancer development and apoptosis. CAS is highly expressed in many types of tumor cell lines and induced proliferation in normal cells (Brinkmann et al., 1995). Previous studies showed that CAS expression has a strong correlation with cancer development and genome instability (Brinkmann, 1998; Brinkmann, 1996; Ried, 1996; Savelieva, 1997; Wellmann, 1997). Interestingly, CAS expression can be induced by several apoptotic stimuli such as tumor necrosis factor, immune toxins (Brinkmann et al., 1995; Brinkmann, 1995, 1996) and lethal dose of UV (data not shown). These apoptotic stimuli may boost apoptosis in tumor cells that highly express CAS via the mechanism we describe above.

While we tried to reconstitute the PHAPI regulatory pathway with identified mediator CAS, we found out that Hsp70 is a critical factor for *in vitro* reconstitution using purified proteins. Previously, we were able to reconstitute apoptosome formation assay without Hsp70 with higher concentration of recombinant Apaf-1. However, to see the effect of PHAPI and CAS, Hsp70 protein was required. The function of Hsp70 in this pathway is still not clear, while the Hsp70 mutant data suggests that Hsp70's substrate binding activity is necessary to carry out its function. We can speculate Hsp70 may chaperon Apaf-1 to facilitate conformational change during this process, as Apaf-1 undergoes dramatic conformational change during apoptosome

assembly. Hsp70 protein is known to be a negative regulator of apoptosome (Beere et al., 2000; Saleh, 2000). However, the concentration of Hsp70 used to see negative effect on apoptosome formation was much higher than endogenous concentration of Apaf-1-associated Hsp70. Whether Hsp70 inhibits apoptosome formation by inhibiting Apaf-1 is not clear with recent study from Steel et al. (Steel, 2004). Moreover, recent findings suggest that Hsp70 may inhibit apoptosis with many different targets such as regulatory proteins upstream of the mitochondria, AIF, or proteins on the lysosomal membrane (Nylandsted, 2004; Ravagnan, 2001; Stankiewicz, 2005; Steel, 2004).

CAS and PHAPI are the first example of nucleotide exchange factor for Apaf-1. There may be more proteins regulate apoptosome formation at the level of nucleotide hydrolysis or exchange on Apaf-1. It seems not likely that CAS and PHAPI are absolutely required for apoptosome formation as we can reconstitute apoptosome formation without PHAPI and CAS. At least in certain cancer cell lines that highly express CAS protein, CAS plays an important role to augment apoptotic response. And our CAS knock down results support this idea. Therefore, it would be interesting to know how CAS is regulated in cells. Previous report shows that the phosphorylation of CAS by MEK1 affects CAS translocation in HeLa cells (Scherf, 1998). The effect of

modification or intracellular translocation of CAS upon apoptotic stimuli in different cancer cells need to be tested. Recent report described unusual sensitivity to cytochrome *c* in breast cancer cell lines that overexpress PHAPI (Schafer, 2006). In these cells CAS must be regulated to act on apoptosome. It would be interesting to compare the cellular property of CAS in these cell lines to other cell lines that are non-sensitive to cytochrome *c*. Furthermore, it is interesting that adding PHAPI to cell lysates from breast cancer cells were sufficient to activate caspase-3 (Schafer, 2006). In our previous study, we showed that prothymosin- α protein had to be removed to see PHAPI mediated caspase activation. It is possible that these breast cancer cells have developed a signaling pathway that can regulate prothymosin- α . It will be critical to study how these cell lines suppress prothymosin- α for better understanding of apoptosome regulation.

Experimental Procedures

Reagents

Nucleotides dATP and dADP were purchased from Amersham Pharmacia; [α -³³P] dATP was obtained from MP Bioscience. Polyclonal antibodies against Apaf-1 was prepared as described (Jiang and Wang, 2000).

The following antibodies were purchased for Western blots: monoclonal anti-CAS (Pharmingen), monoclonal anti-Hsp70 (Pharmingen), and polyclonal anti-Actin antibody (Sigma). siRNA double strand oligos against CAS (Set I GCCATCTACCTAGTGACAT, Set II GTCCTCCGTACAGCACATT) were synthesized by Dharmacon.

Protein purification for in vitro assays

Recombinant Apaf-1 was expressed in insect sf21 cells and purified as described (Kim et al., 2005). Endogenous Apaf-1 was purified from HeLa S-100 followed by sequence of Q-sepharose column, Ammonium Sulfate precipitation (40 %), Hitrap Q, Heparin and Mono Q columns using a fast protein liquid chromatography (FPLC) system (Amersham Pharmacia). Recombinant procaspase-9 and procaspase-3 were expressed and purified as described (Jiang and Wang, 2000), followed by nickel affinity purification and a Hitrap Q column purification. Purified horse cytochrome *c* was prepared as described (Liu et al., 1996), followed by Mono S purification using SMART system (Amersham Pharmacia). Recombinant PHAPI and ProT were expressed in bacteria and purified as described (Jiang et al., 2003), using nickel affinity purification and Hitrap Q purification. CAS cDNA was provided from Dr. Görlich lab (Kutay et al., 1997), and was cloned into modified pFastBac-HTB (C-terminal with Flag tag and 9 histidines). Then, the plasmid was used

to make baculovirus, and recombinant CAS was expressed in sf21 cells after infection with baculovirus according to the manufacturer's instruction. Recombinant CAS was expressed and purified by nickel affinity purification, followed by precipitation with 40 % of ammonium sulfate, gel filtration on Superdex 200 and Hitrap Q column purification. Hsp70 cDNA was cloned into pET15b vector with N-terminal 6-Histidines. Hsp70 mutant (Hsp70AAAA) was cloned in to the same vector using full length Hsp70 cDNA as a template. 4 amino acids at the C-terminal end were changed to 4 alanine residues using a QuickChange Site-Directed Mutagenesis kit (Stratagene). Recombinant Hsp70 and Hsp70AAAA were expressed in bacteria and purified with nickel affinity column and Hitrap Q column.

Fluorogenic assay for caspase-3 activity

Caspase-3 activity was measured using 10 μ M of fluorogenic DEVD substrate (Calbiochem). Samples were transferred to 384-well plate, caspase-3 activity was measured by using XFluor4 spectrometry reader (Tecan) (Kim et al., 2005). In brief, 15 nM of recombinant Apaf-1 (or 15 nM of endogenous Apaf-1 in the initial assays), 20 nM of Procaspase-9, 50 nM of Procaspase-3, 50 nM of cytochrome *c*, 5 μ M of dATP, 300 nM of PHAPI, 50 nM of CAS, 2 μ M of Prothymosin- α , 50 nM of Hsp70 or Hsp70AAAA, 0.2 mM of PETCM (Jiang et al., 2003) and 10 μ M of fluorogenic DEVD substrate were used for in

vitro assay with buffer A supplied with 2.5 mM of MgCl₂. The assay was performed at 30 °C in 20 µl final volume.

Purification and identification of CAS

All purification steps were carried out at 4 °C, using a FPLC system (Amersham Pharmacia). HeLa cell S-100 was prepared as described (Liu et al., 1996), using Buffer A (20 mM Hepes, pH 7.5, 10 mM KCl, 1.5 mM MgCl₂, 1 mM EDTA, 1 mM EGTA, 1 mM DTT, and 0.1 mM PMSF) containing protease inhibitors (Roche). 250 mg of HeLa S-100 was applied to a Q-sepharose column equilibrated with buffer A (60 ml bed volume) and Apaf-1 containing fractions were collected. Apaf-1 fractions were precipitated with 40% of ammonium sulfate. Supernatant was used for purifying endogenous Apaf-1, and the precipitates were resuspended with Buffer A and filtered using 0.45µm syringe filters (Nalgene) before loading to the next column. The resuspended precipitates were loaded on Superdex 200 gel filtration column, and the fractions with PHAPI responsive activity were collected. The activity flew through Heparin column. The flow-through of Heparin column was incubated with recombinant Apaf-1 (1 µg/ml) for 2 hours, then applied to Heparin column again. The recombinant Apaf-1 was eluted with increasing concentration of NaCl, and co-eluted proteins were visualized by silver

staining (Invitrogen). The purified proteins were identified as CAS by Mass-Mass spectrum analysis.

CAS RNAi

HeLa cells were transfected by siRNA against CAS to knock down CAS expression using Lipofectamine 2000 according to the manufacturer's instruction. After transient transfection with siRNA, HeLa cells were harvested to prepare S-100. The S-100 from control or CAS RNAi cells, were applied to Hitrap-Q column to fractionate Apaf-1. The Apaf-1 containing fractions were pooled and used for in vitro assay.

To generate inducible CAS shRNA cell line, the set I sequence (GCAGCCATCTACCTAGTGACAT) oligo was annealed following the protocol from Oligoengine and cloned into BglII and HindIII sites of pSuperior.puro vector (Oligoengine) to generate 6 copies of H1 promoter + shRNA cassette as previously described (Zhong, 2005). The CAS shRNA construct was transfected to tetracycline repressor-expressing HT-29 stable cell line grown in Macoy's 5 media with tetracycline-free 10% FBS. The next day, transfected cells were selected against 10 µg/ml blasticidine and 1 µg/ml puromycin. After 2-3 weeks, the individual colonies were picked and tested for CAS shRNA expression. Clones were treated with 1 µg/ml tetracycline for 72 hours to check the expression of CAS protein. For the rescue experiments, full-

length CAS with RNAi-resistant scrambled-silent mutations at the shRNA (Set I) complementary sequence were generated (from GCAGCCATCTACCTAGTGACAT to GCAGCAATATACCTTGTGACTT) using a QuickChange Site-Directed Mutagenesis kit. The RNAi-resistant CAS sequence was cloned into pCI/Neo vector with C-terminal 3XFlag tag, and transfected to the tetracycline repressor/CAS shRNA stable cell lines. 6 hours after transfection, the media was replaced with media containing 1 µg/ml tetracycline. 48 hours later, cells were treated with 100 mJ/cm² of UV light using UV Stratalinker 1800 (Stratagene), and cell death was assessed after 24 hours.

Cell death quantification

Cells were washed 3 times with chilled PBS at the indicated time after treatment, and stained with 2% of methylene blue in 50% of ethanol for 15 minutes at room temperature. Then, gently washed the plate with distilled water for 10 times and dried it. Methylene blue would stain the attached live cells. Then, extracted the dye with 1% SDS solution and read OD at 640 nm to quantify surviving cells.

dATP loading assay

dATP loading to Apaf-1 was measured using [α -³³P] dATP (3000 Ci/mM). 10 µCi of [α -³³P] dATP was added to the assay mixture described

earlier, with 5 μ M of cold dATP in 20 μ l final volume. The samples were incubated at 30 °C. At the indicated time point, the samples were diluted with 100 μ l of chilled buffer A containing additional 100 mM of NaCl and applied to desalting column twice to get rid of unbound free dATP.

Then, samples were concentrated using Microcon (Millipore) approximately to 10 μ l. 3 μ l of each samples were spotted on PEI cellulose TLC plate and separated in the separation buffer (1 M formic acid, 0.5 M LiCl). The TLC plate was dried and exposed to BAS-III plate (Fuji).

Then, visualized and quantified by Typhoon PhosphorImager and IMAGEQUANT software (Molecular Dynamics). On the other hand, using different concentration s of dATP, dATP loaded Apaf-1 was measured using quick filter binding assay (Jiang and Wang, 2000). In this assay, radioactive dATP was added to 1/ 100 of each indicated concentration of cold dATP with other components indicated in the final volume of 20 μ l. After 60 minutes of incubation, samples were diluted with 500 μ l of chilled washing buffer (20 mM Tris-Cl, pH 8.0, 100 mM NaCl, and 40 mM MgCl₂) and filtered through 25-mm BA85 nitrocellulose filters (Schleicher and Schuell). Filters were washed twice with 2 ml of chilled washing buffer and exposed to BAS-III plate (Fuji), then quantified using Typhoon PhosphorImager and

IMAGEQUANT software. Values were plotted V_{\max} (intensity/min) over [dATP] and K_s were calculated by best-fit method.

Figure 1.

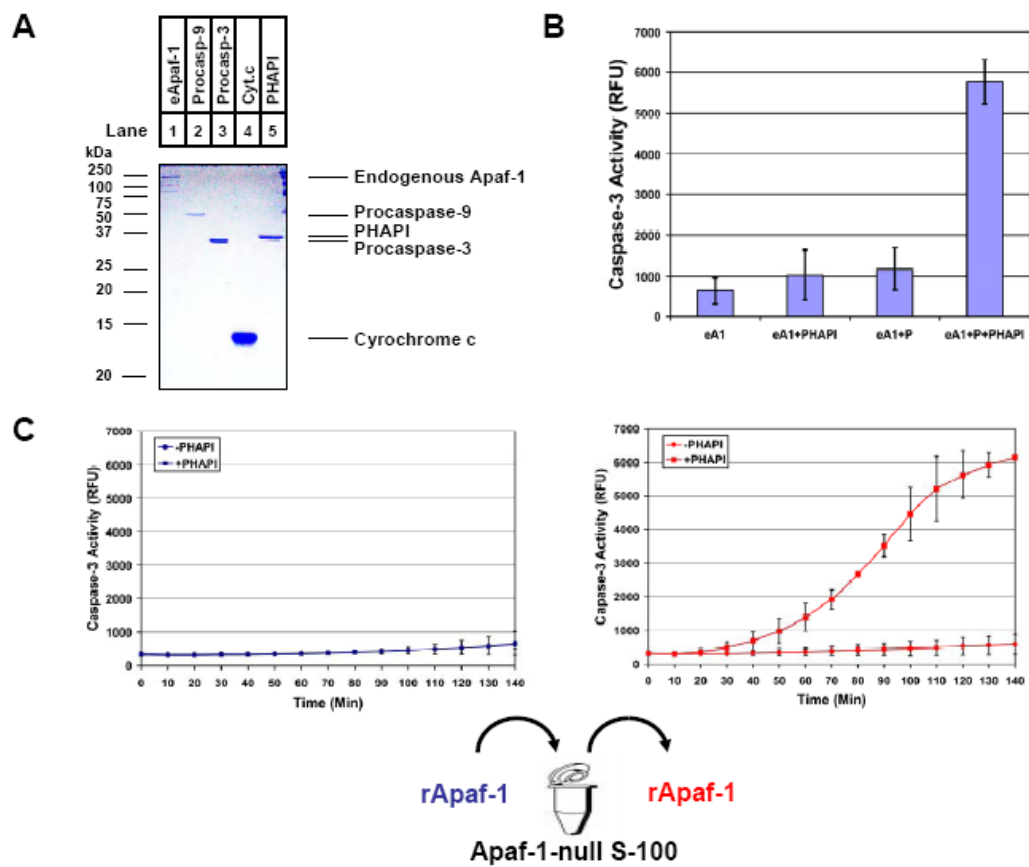


Figure 4-1. Cell-free Assay for Identifying Mediator of PHAPI
(A) Coomassie blue staining of purified proteins used in assay. eApaf-1; purified endogenous Apaf-1 (0.5 μ g), Procasp-9 and Procasp-3; purified recombinant procaspase-9 and procaspase-3 (0.5 μ g each), Cyt.c; purified bovine cytochrome *c* (1 μ g), PHAPI; purified recombinant PHAPI (0.5 μ g). 8 % of SDS polyacrilamide gel was used to separate proteins (B) Fluorogenic DEVD substrate cleaving activity assay by caspase-3. Aliquots of starting material (P; 40% ammonium precipitates of Apaf-1-containing Q column elutes) for biochemical purification were used to see caspase-3 activation by PHAPI. Assay mixture included purified endogenous Apaf-1 (eA1), cytochrome *c*, dATP, procaspase-9 and procaspase-3. Caspase-3 activity was measured in the presence or absence of PHAPI or P. (C) Recombinant Apaf-1 was incubated with Apaf-1-null MEF cell extract (S-100) or buffer A at 4 $^{\circ}$ C for 2 hours and re-purified using nickel beads. Caspase-3 activity was measured after re-purification of Apaf-1 from bufferA (left) or Apaf-1-null MEF S-100 (right). The data represent the average fluorescence reading and standard deviation of two independent experiments at 90 minutes at 30 $^{\circ}$ C.

Figure 2.

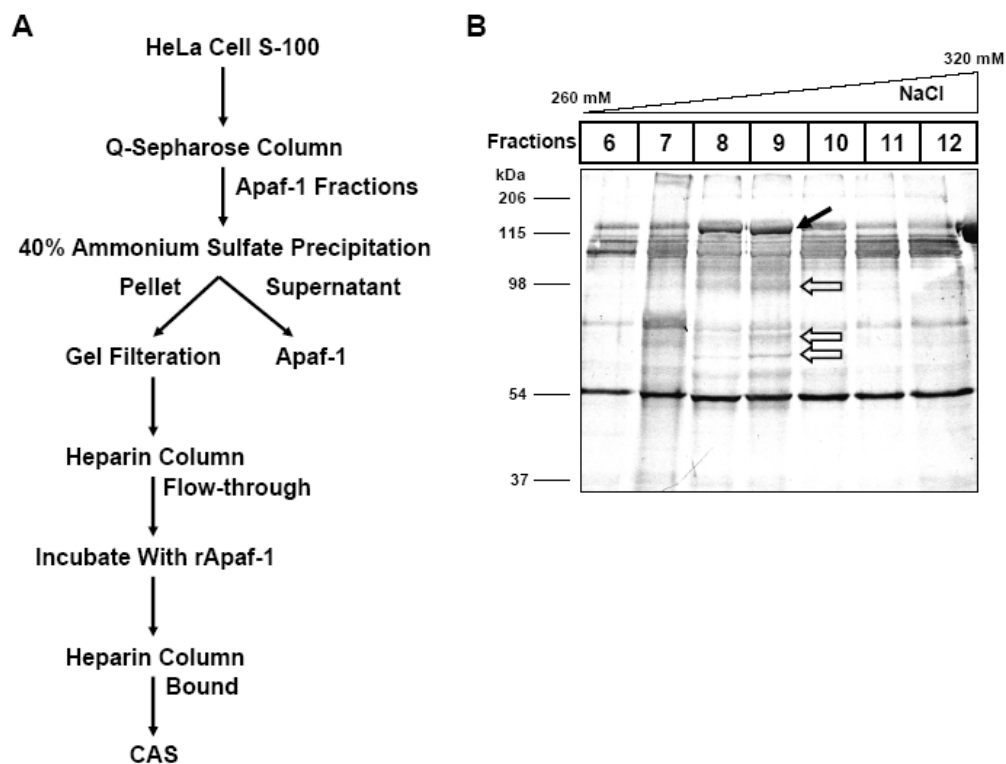


Figure 4-2. Purification of PHAPI Mediator

(A) Diagram of purification scheme for PHAPI mediator. See the Experimental Procedures and Results for details. (B) Silver staining at the final step of purification. Aliquots of 20 μ l of fractions from the last Heparin column were applied to 10% of SDS-PAGE followed and silver stained (Invitrogen). Black arrow indicates recombinant Apaf-1. White arrows indicate co-migrating bands with Apaf-1 through Heparin column (Fractions 8 and 9). See details in Experimental Procedures.

Figure 3.

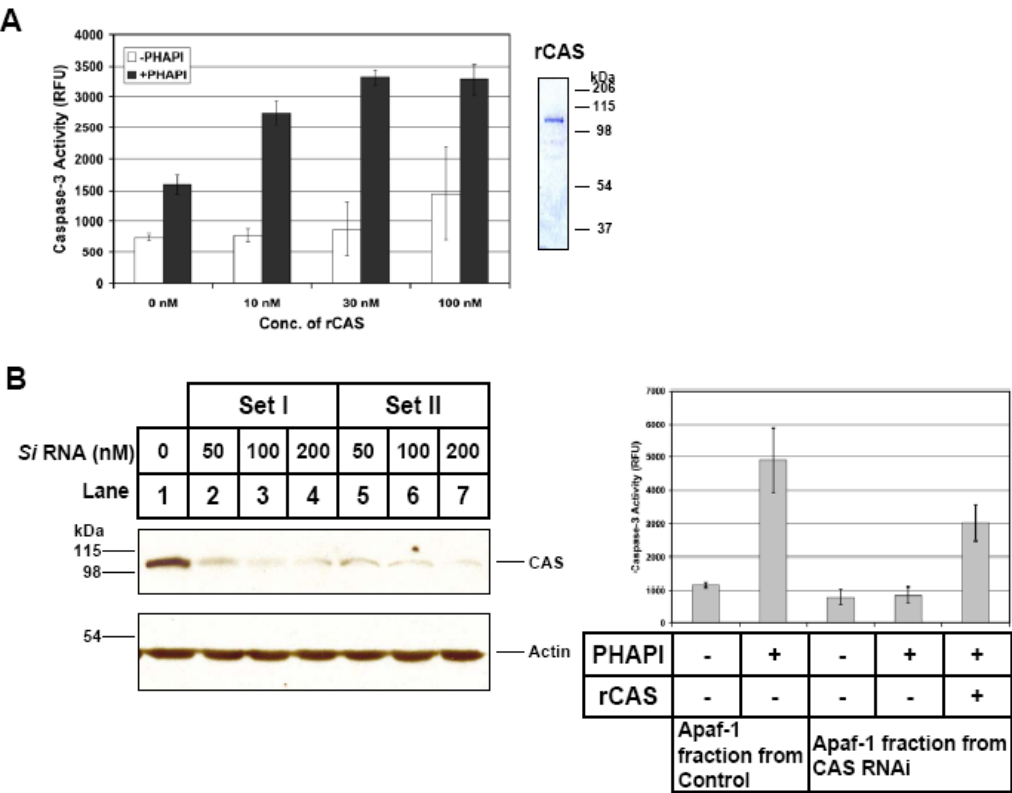


Figure 4-3. Reiteration of Assay using Recombinant CAS
(A) Titration of recombinant CAS. Caspase-3 activity was measured using indicated concentration of recombinant CAS (rCAS) in the presence or absence of PHAPI. 1 μ g of purified recombinant CAS was applied to 10% SDS-PAGE followed by coomassie blue staining. (B) HeLa cells were transfected with indicated concentration of siRNA against CAS. HeLa cells were harvested after 48hrs to prepare S-100. (Left panel); Western blotting against CAS was performed with 20 μ g of S-100 from each sample. Then, using the same blot, antibody against actin was re-probed for loading control. (Right panel); The HeLa cell S-100 from control RNAi (lane 1) and SetI (lane 3; 100 nM) RNA were applied to Hitrap Q to fractionate endogenous Apaf-1. Aliquots of 6 μ l of Apaf-1 fraction were incubated with cytochrome *c*, dATP, procaspase-9 and procaspase-3. Caspase-3 activity was measured in the presence of absence of PHAPI in the assay mixture. 50 nM of recombinant CAS was added to the mixture at the last column in the graph. The data represent the average fluorescence reading and standard deviation of two independent experiments at 90 minutes at 30 $^{\circ}$ C.

Figure 4.

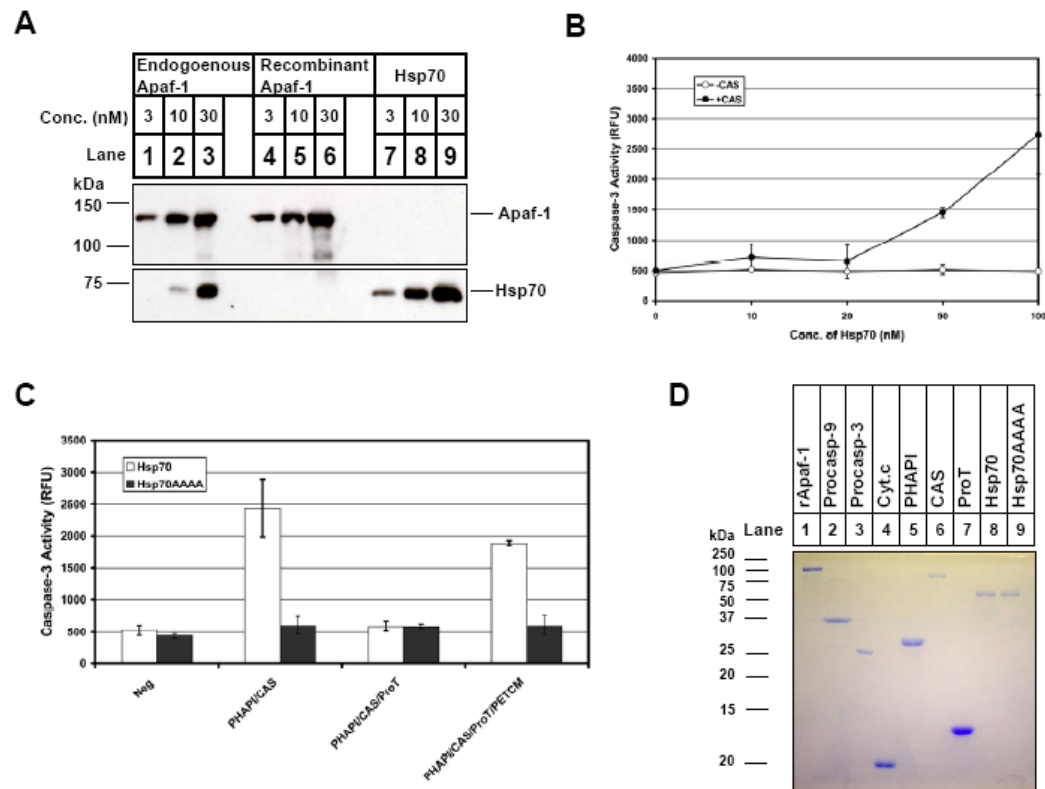


Figure 4-4. In vitro Reconstitution of Apoptosome Regulatory Pathway

(A) 30 μ l of aliquots from the indicated concentrations of endogenous Apaf-1 (lane 1-3), recombinant Apaf-1 (lane 4-6) and recombinant Hsp70 (lane 7-9) were subjected to western blotting for Apaf-1 and Hsp70. Hsp70 protein was associated with purified endogenous Apaf-1 but not with recombinant Apaf-1. (B) Titration of Hsp70. Indicated concentrations of recombinant Hsp70 was used in the reconstitution assay in the absence or presence of CAS and Caspase-3 activity was measured. (C) Total reconstitution assay using Hsp70 or Hsp70AAAA mutant. The assay mixture included recombinant Apaf-1, cytochrome *c*, dATP, procaspase-9, procaspase-3 and Hsp70 or Hsp70AAAA. The indicated additional proteins or a small molecule were added to the mixture and caspase-3 activity was measured. See the Experimental Procedures for details. The purified proteins were visualized by coomassie staining in (D).

The data represent the average fluorescence reading and standard deviation of two independent experiments at 90 minutes at 30 $^{\circ}$ C.

Figure 5.

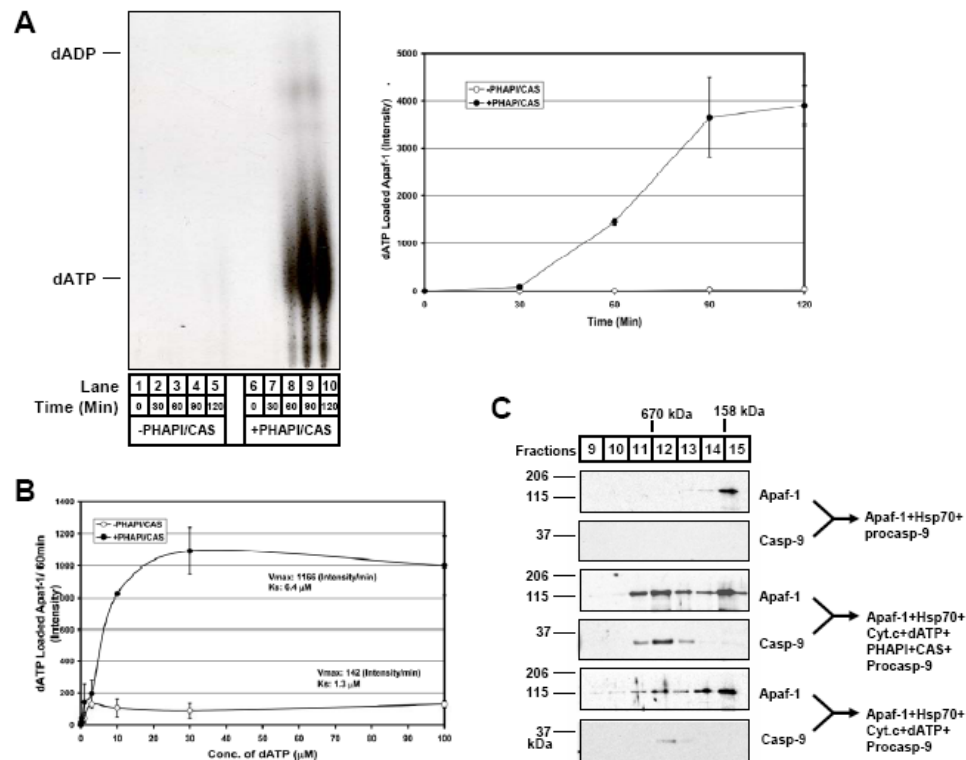


Figure 4-5. CAS and PHAPI Enhance Nucleotide Exchange on Apaf-1 to Facilitate Apoptosome Formation

(A) Radiolabeled dATP loading to Apaf-1 was measured at the indicated time in the presence (lane 6-10) or absence (lane 1-5) of PHAPI and CAS. Loaded dATP was visualized on the film after developing TLC plate. The volume quantification arbitrary unit (Intensity) was plotted at the right panel. (B) K_s of Apaf-1-dATP complex formation was measured at 60 minutes when dATP loading as the linear range using filter binding assay. Volume quantification arbitrary unit (Intensity) was plotted over conc. of dATP. V_{max} was enhanced with PHAPI and CAS. See the Experimental Procedures for details. (C) Apoptosome formation was visualized by western blotting of Apaf-1 after gel filtration column. Indicated mixture was incubated at 30 °C for 1 hour before subjected to superpose 6 gel filtration column. Apoptosome runs in fraction 11 and 12. The monomer Apaf-1 is in fraction 15. Western blot of active caspase-9 (35 kDa) is shown under each Apaf-1 blot.

The data represent the average dATP loading and standard deviation of two independent experiments.

Figure 6.

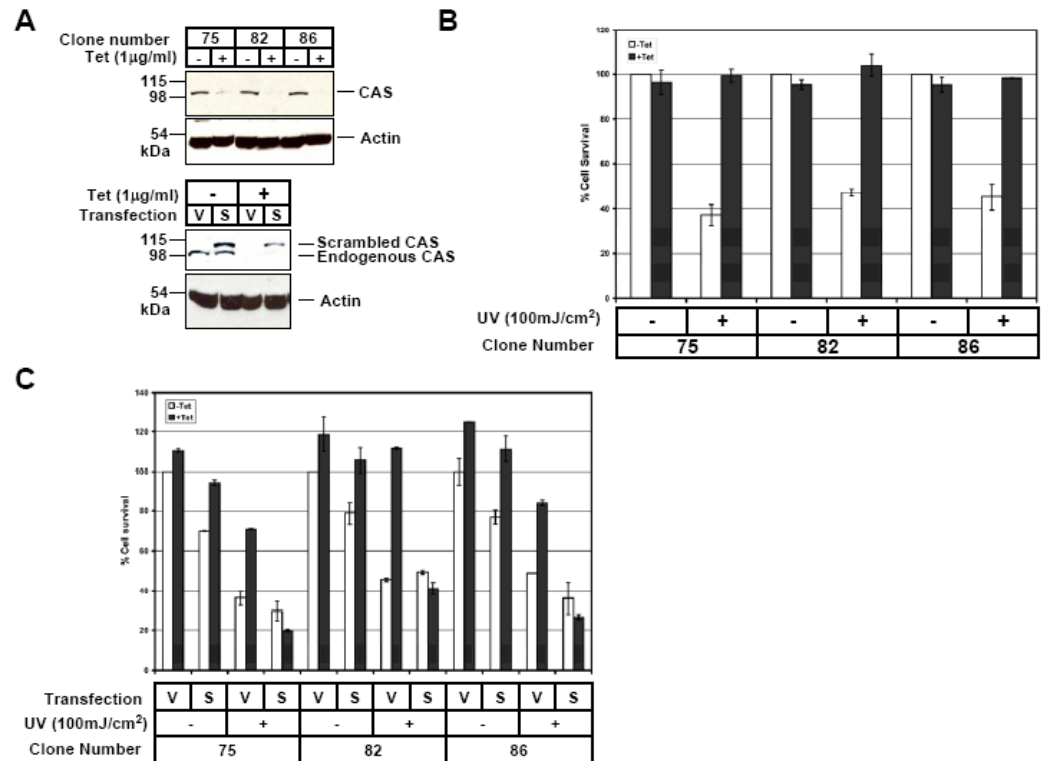


Figure 4-6. Inducible knock-down of CAS shRNA

(A) All three clones successfully knocked down CAS expression when tetracycline was added (upper panel). Actin western blot is shown for loading control. Lower panel; RNAi-resistant scrambled CAS was transfected to rescue the cell death phenotype. Scrambled CAS maintained its expression with tetracycline treatment while endogenous CAS was knocked down. V; vector plasmid, S; scrambled CAS plasmid. (B) Tetracycline (Tet) inducible CAS knock-down in HT-29 cells. Three clones (75, 82 and 86) were picked to measure cell survival after 24 hours of UV treatment. Lethal dose of UV caused cell death in non-induced cells but CAS shRNA-induced cells were resistant to UV treatment. Knock-down level of CAS is shown in (A). (C) Rescue cell death phenotype by overexpressing RNAi resistant CAS. 24 hours after transfection of either vector (V) or scrambled CAS (S) plasmids, tetracycline was added to culture media. After 48 hours, cells were treated with UV for 24 hours, then, cell survival was measured. Overexpression of RNAi-resistant scrambled CAS restored UV sensitivity in HT-29 cells.

The data represent the average percentage of cell survival and standard deviation of two independent experiments.

Summary

My thesis study has been investigating the biochemistry of apoptosome-mediated caspase activation. The small molecule PETCM activated caspase-3 by inactivating the inhibitory function of prothymosin- α on apoptosome formation. Prothymosin- α inhibited apoptosome formation possibly by interfering with cytochrome *c* binding or initial nucleotide hydrolysis on Apaf-1. The precise target of prothymosin- α affecting apoptosome formation could be tested by analyzing its interaction with cytochrome *c* or Apaf-1 and nucleotide hydrolysis. Knock-down of prothymosin- α expression in HeLa cells resulted in sensitizing cells to low-dose of UV treatment. Since prothymosin- α protein is overexpressed in cancer cell lines, we could speculate its oncogenic function might be through preventing apoptosis. Also it would be interesting to find out how the small molecule PETCM regulates the function of prothymosin- α . Target of the small molecule PETCM still remains to be determined. The apoptotic stimuli must inactivate prothymosin- α to form apoptosome. Thus, next critical question to ask is whether there is a cellular signaling pathway to regulate prothymosin- α in response to apoptotic stresses.

On the other hand, PHAP proteins positively regulated apoptosome function. The PHAPI stimulated caspase-9 activation by either loading more caspase-9 or facilitating caspase-9 activation step in partially purified Q30 system. However, how it carries out its function on apoptosome was not clear until we identified its mediator. We identified CAS as a mediator of PHAPI using biochemical fractionation. PHAPI and CAS stimulated apoptosome formation by enhancing nucleotide exchange on Apaf-1. PHAPI has a tumor suppressive ability, which is consistent with its pro-apoptotic function. PHAPI expression is lost in certain prostate cancer tissues. Unlike PHAPI, CAS has functions in both cell proliferation and cell death. CAS overexpression is observed in different cancer cell lines while knock down of CAS expression switches cells to be resistant to apoptotic stimuli. The detailed molecular mechanism how PHAPI and CAS cooperatively regulate apoptosome formation remains to be determined.

As a result of analyzing apoptosome formation using purified recombinant Apaf-1, we discovered that the recombinant Apaf-1 obtained from the insect cell expression system was bound to dATP. The bound dATP were hydrolyzed upon cytochrome *c* binding, suggesting that cytochrome *c* may serve as a dATPase activation factor. Recently, Riedl et al. (2005) showed that the WD-40-deleted Apaf-1 is bound to ADP implying that ADP molecule is an

organizing center for locking Apaf-1 conformation as an inactive form. WD-40-deleted Apaf-1 was active in their ATPase assay consistent with our result using full-length Apaf-1 in the presence of cytochrome *c*. To form an active apoptosome, nucleotide exchange was required. The data obtained in chapter 3 shows that there is only one round of nucleotide hydrolysis during apoptosome formation. However, the previous work from our lab using non-hydrolysable nucleotide analogs AMP-PCP and ATP- γ S generated contradictory results. The dATP/ATP was replaceable with AMP-PCP in apoptosome formation, while ATP- γ S inhibited apoptosome formation. To resolve this confusion, we could use the ATPase-dead mutant of Apaf-1 to measure the apoptosome formation. The procaspase-9 recruitment to the apoptosome slightly changed the structure of apoptosome (Acehan et al. 2002, and Figure 7 in Chapter 1). The CARD domain and ATPase regions of the hub protruded more when apoptosome is incubated with noncleavable procaspase-9. Thus, it is possible that the structure differences in apoptosome before and after caspase-9 recruitment could affect the ATPase activity of apoptosome. In chapter 3, only Apaf-1, cytochrome *c*, and dATP were incubated to measure nucleotide hydrolysis. To test the hypothesis above, we could measure nucleotide hydrolysis in the presence of procaspase-9 and/or caspase-3.

Our study provides an insight to understand the biochemistry of apoptosome in more detail. The regulation of apoptosome formation and its function is one of the most important steps during apoptosis.

References

- Acehan, D., Jiang, X., Morgan, DG., Heuser, JE., Wang, X., Akey, CW. (2002). *Mol Cell*. 9, 423-432.
- Adams, JM., Cory, S. (1998). *Science*. 281,1322-1326.
- Adrain, C., Brumatti, G., and Martin, SJ. (2006). *Trends Biochem Sci*. 31, 243-247.
- Adrain, C., Slee, E. A., Harte, M. T. & Martin, S. J. (1999) *J. Biol. Chem*. 274, 20855–20860.
- Alnemri, E. S., Livingston, D. J., Nicholson, D. W., Salvesen, G., Thornberry, N. A., Wong, W. W. & Yuan, J. (1996) *Cell* 87, 171
- Bai, J., Brody, JR., Kadkol, SS., Pasternack, GR. (2001). *Oncogene*. 20, 2153-60.
- Baud, V., and Karin, M (2001). *Trends Cell Biol*. 11, 372-377
- Beere HM. (2005). *J Clin Invest*. 115, 2633-2639.
- Beere, H., Wolf, B., Cain, K., Mosser, D., Mahboubi, A., Kuwana, T., Tailor, P., Morimoto, R., Cohen, G., and Green, D. (2000). *Nat Cell Biol* 2, 469-475.
- Behrens, P., Brinkmann, U., and Wellmann, A. (2003). *Apoptosis* 8, 39-44.

Benedict, MA., Hu, Y., Inohara, N., Nunez, G. (2000). *J Biol Chem* 275, 8461-8468.

Brinkmann, U. (1998). *Am J Hum Genet* 62, 509–513.

Brinkmann, U., Brinkmann, E., and Pastan, I. (1995). *Mol Med* 1, 206–216.

Brinkmann, U., Brinkmann, E., Gallo, M., and Pastan, I. (1995). *Proc Natl Acad Sci U S A* 92, 10427-10431.

Brinkmann, U., Brinkmann, E., Gallo, M., Scherf, U., Pastan, I. (1996). *Biochemistry* 35, 6891–6899.

Brody, JR., Kadkol, SS., Mahmoud, MA., Rebel, JM., Pasternack, GR. (1999). *J Biol Chem.* 274, 20053-5.

Bruey, JM., et al. (2000). *Nat Cell Biol* 2, 645-652.

Cain, K., Bratton, S. B., Langlais, C., Walker, G., Brown, D. G, Sun, X. M. & Cohen, G. M. (2000) *J. Biol. Chem.* 275, 6067–6070.

Cecconi, F., Alvarez-Bolado, G., Meyer, BI., Roth, KA., Gruss, P. (1998). *Cell.* 94, 727-737.

Chao, DT., Korsmeyer, SJ. (1998). *Annu Rev Immunol.* 16, 395-419.

Chen, M., and Wang, J. (2002). *Apoptosis.* 7, 313-319.

Chen, TH., Brody, JR., Romantsev, FE., Yu, JG., Kayler, AE., Voneiff, E., Kuhajda, FP., Pasternack, GR. (1996). *Mol Biol Cell.* 7, 2045-56.

Chew, S. K., Akdemir, F., Chen, P., Lu, W. J., Mills, K., Daish, T., Kumar, S., Rodriguez, A. & Abrams, J. M. (2004) *Dev. Cell* 7, 897–907.

Daish, T. J., Mills, K., Kumar, S. (2004) *Dev. Cell* 7, 909–915.

Degterev, A., Boyce, M., Yuan, J. (2003). *Oncogene*. 22, 8543-8567.

Deveraux, QL., Reed, JC. (1999). IAP family proteins-suppressors of apoptosis. *Genes Dev.* 13, 239-252.

Deveraux, QL., Roy, N., Stennicke, HR., et al. (1998). *EMBO J* 17, 2215-2223.

Dosil, M., Alvarez-Fernandez, L., Gomez-Marquez, J. (1993). *Exp Cell Res.* 204, 94-101.

Du, C., Fang, M., Li, YC., Li, L., Wang, XD. (2000). *Cell.* 102, 33-42.

Eguchi, Y., Shimizu, S., and Tsujimoto, Y. (1997). *Cancer Res* 57, 1835-1840.

Eguchi, Y., Srinivasan, A., Tomaselli, K., Shimizu, S., and Tsujimoto, Y. (1999). *Cancer Res* 59, 2174-2181.

Eilers, M., Schirm, S., Bishop, JM. (1991). *EMBO J.* 10, 133-141.

Freeman, B., Myers, M., Schumacher, R., and Morimoto, R. (1995). *EMBO J* 14, 2281-2292.

Fu, WN., Kelsey, SM., Newland, AC., Jia, L. (2001). *Biochem Biophys Res Commun* 282, 268-272.

Gabai, VL., Mabuchi, K., Mosser, DD., Sherman, MY. (2002), *Mol Cell Biol.* 22, 3415-3424.

- Goldstein, JC., Waterhouse, NJ., Juin, P., Evan, GI., Green, DR.. (2000). *Nat Cell Biol.* 2, 156-162.
- Gotoh, T., Terada, K., Oyadomari, S., Mori M. (2004). *Cell Death Diff.* 11, 390-402.
- Gross, A., McDonnell, J., and Korsmeyer, S. (1999). *Genes Dev* 13, 1899-1911.
- Hahn, C., Hirsch, B., Janke, D., Durkop, H., Stein, H. (1999). *Biochem Biophys Res Commun* 261, 746-749.
- Hakem, R., Hakem, A., Duncan, G. S., Henderson, J. T., Woo, M., Soengas, M. S., Elia, A., de la Pompa, J. L., Kagi, D., Khoo, W., et al. (1998) *Cell* 94, 339–352.
- Hegde, R., Srinivasula, SM., Zhang, Z., Wassell, R., Mukattash, R., Cilenti, L., DuBois, G., Lazebnik, Y., Zervos, AS., Fernandes-Alnemri, T., Alnemri, ES. (2002). *J Biol Chem.* 277, 432-8.
- Hill, M., Adrain, C., Duriez, PJ., Creagh, EM., Martin, SJ. (2004). *EMBO J* 23, 2134-2145.
- Inohara, N., Ogura, Y. & Nunez, G. (2002) *Curr. Opin. Microbiol.* 5, 76–80.
- Jiang, M., Lin, T., Lee, T., Huang, H., Lin, C., and Liao, C. (2001). *Mol Cell Biol Res Commun* 4, 353-358.
- Jiang, X., and Wang, X. (2000). *J Biol Chem* 275, 31199-31203.

Jiang, X., Kim, H.-E., Shu, H., Zhao, Y., Zhang, H., Kofron, J., Donnelly, J., Burns, D., Ng, S.-c., Rosenberg, S., et al. (2003). *Science* 299, 223 - 226.

Jiang, X., Kim, H.-E., Shu, H., Zhao, Y., Zhang, H., Kofron, J., Donnelly, J., Burns, D., Ng, S.-C., Rosenberg, A. and Wang, X. (2003) *Science* 299, 223–226.

Kanuka, H., Sawamoto, K., Inohara, N., Matsuno, K., Okano, H. & Miura, M. (1999) *Mol. Cell* 4, 757–769.

Kim, H.-E., Du, F., Fang, M., and Wang, X. (2005). *Proc Natl Acad Sci USA* 102 17545-17550

Kronbluth, S., White, K. (2005). *J Cell Sci.* 118, 1779-1787.

Kuida, K., Haydar, T. F., Kuan, C. Y., Gu, Y., Taya, C., Karasuyama, H., Su, M. S., Rakic, P. & Flavell, R. A. (1998) *Cell* 94, 325–337.

Kuida, K., Zheng, T. S., Na, S., Kuan, C., Yang, D., Karasuyama, H., Rakic, P. and Flavell, R. A. (1996) *Nature* 384, 368–372.

Kutay, U., Bischoff, F.R., Kostka, S., Kraft, R., and Görrlich, D. (1997). *Cell* 90, 1061–1071.

Leoni, L. M., Chao, Q., Cottam, H. B., Genini, D., Rosenbach, M., Carrera, C. J., Budihardjo, I., Wang, X. & Carson, D. A. (1998) *Proc. Natl. Acad. Sci. USA* 95, 9567–9571.

Li, LY., Luo, X., Wang, X. (2001). *Nature.* 412, 95-99.

- Li, M., Makkinje, A., Damuni Z. (1996). *Biochemistry*. 35, 6998-7002.
- Li, P., Nijhawan, D., Budihardjo, I., Srinivasula, S. M., Ahmad, M., Alnemri, E. S. and Wang, X. (1997) *Cell* 91, 479–489.
- Li, P., Nijhawan, D., Budihardjo, I., Srinivasula, S., Ahmad, M., Alnemri, E., and Wang, X. (1997). *Cell* 91, 479-489.
- Liu, X., Kim, C., Yang, J., Jemmerson, R., and Wang, X. (1996). *Cell*. 86, 147-157.
- Magdalena, C., Dominguez, F., Loidi, L., Puente, JL. (2000). *Br J Cancer*. 82, 584-590
- Martinon, F., Burns, K. & Tschopp, J. (2002) *Mol. Cell* 10, 417–426.
- Martinou, J., Green, DR. (2001). *Nat Rev Mol Cell Biol* 2, 63-37.
- Matilla, A., Koshy, BT., Cummings, CJ., Isobe, T., Orr, HT., Zoghbi, HY. (1997). *Nature*. 389, 974-8.
- Matsuoka, K., Taoka, M., Satozawa, N., Nakayama, H., Ichimura, T., Takahashi, N., Yamakuni, T., Song, SY., Isobe, T. (1994). *Proc Natl Acad Sci U S A*. 91, 9670-9674.
- Meier, P., Finch, A., Evan, G. (2000). *Nature*. 407, 796-801.
- Mencinger, M., Panagopoulos, I., Contreras, JA., Mitelman, F., Aman, P. (1998). *Biochim Biophys Acta*. 1395, 176-80.

Mesner, PW Jr., Bible, KC., Martins, LM., Kottke, TJ., Srinivasula, SM., Svingen, PA., Chilcote, TJ., Basi, GS., Tung, JS., Krajewski, S., Reed, JC., Alnemri, ES., Earnshaw, WC., Kaufmann, SH. (1999). *J Biol Chem.* 274, 22635-22645.

Mutai, H., Toyoshima, Y., Sun, W., Hattori, N., Tanaka, S., Shiota, K. (2000). *Biochem Biophys Res Commun.* 274, 427-433.

Nagata, S. (1999). *Annu Rev Genet* 33:29-55., 29-55.

Nylandsted, J., Gyrd-Hansen, M., Danielewicz, A., Fehrenbacher, N., Lademann, U., Hoyer-Hansen, M., Weber, E., Multhoff, G., Rohde, M., Jaattela, M. (2004). *J Exp Med* 200, 425-435.

Orre, RS., Cotter, MA 2nd., Subramanian, C., Robertson, ES. (2001). *J Biol Chem.* 276, 1794-1799.

Pandy, P., Saleh, A., Nakazawa, A., et al. (2000). *EMBO J* 19, 4310-4322.

Parrish, J., Li, L., Klotz, K., Ledwich, D., Wang, X., Xue, D. (2001). *Nature.* 412, 90-94.

Paul, C., Manero, F., Gonin, S., Kertx-remy, C., Virost S., Arrigo, AP. (2002). *Mol Cell Biol.* 22, 816-834.

Pineiro, A., Cordero, OJ., Nogueira, M. (2000). *Peptides.* 21, 1433-1446.

Sburlati, AR., Manrow, RE., Berger, SL. (1991). *Proc Natl Acad Sci U S A.* 88, 253-257.

Radrizzani, M., Vila-Ortiz, G., Cafferata, EG., Di Tella, MC., Gonzalez-Guerrico, A., Perandones, C., Pivetta, OH., Carminatti, H., Idoyaga, Vargas VP., Santa-Coloma, TA. (2001). *Brain Res.* 907, 162-174.

Ravagnan, L., Gurbuxani, S., Susin, SA., Maisse, C., Daugas, E., Zamzami, N., Mak, T., Jaattela, M., Penninger, JM/, Garrido, C., Kroemer, G. (2001). *Nat Cell Biol* 3, 839-843.

Ried, T., Knutzen, R., Steinbeck, R., Blegen, H., Schrock, E., Heselmeyer, K., du Manoir, S., et al (1996). *Genes Chromosom Cancer* 15, 234–245

Riedl, S. J., Li, W., Chao, Y., Schwarzenbacher, R. & Shi, Y. (2005) *Nature* 434, 926–933.

Rodriguez, A., Oliver, H., Zou, H., Chen, P., Wang, X. & Abrams, J. M. (1999) *Nat. Cell Biol.* 1, 272–279.

Rodriguez, J., Lazebnik, Y. (1999). *Genes Dev.* 13, 3179-3184.

Rodriguez, P., Vinuela, JE., Alvarez-Fernandez, L., Buceta, M., Vidal, A., Dominguez, F., Gomez-Marquez, J. (1998). *Biochem J.* 331, 753-761.

Saleh, A., Srinivasula, SM., Balkir, L., Robbins, PD., Alnemri, ES. (2000). *Nat Cell Biol* 2, 476-483.

Savelieva, E., Belair, CD., Newton, MA., DeVries, S., Gray, JW., Waldman, F., Reznikoff, CA. (1997). *Oncogene* 14.

Savill, J., Fadok V. (2000). *Nature.* 407, 784-788.

Schafer, Z., Kornbluth, S. (2006). *Dev Cell*. 10, 549-561.

Schafer, Z., Parrish, AB., Wright, KM., Margolis, SS., Marks, JR., Deshmukh, M., Kornbluth, S. (2006). *Cancer Res* 66, 2210-2218.

Scherf, U., Kalab, P., Dasso, M., Pastan, I., Brinkmann, U. (1998). *Biochem Biophys Res Commun* 250, 623-628.

Seo, SB., McNamara, P., Heo, S., Turner, A., Lane, WS., Chakravarti, D. (2001). *Cell*. 104, 119-130.

Shi, Y. (2002) *Mol. Cell* 9, 459–470.

Smith, MR., al-Katib, A., Mohammad, R., Silverman, A., Szabo, P., Khilnani, S., Kohler, W., Nath, R., Mutchnick, MG. (1993). *Blood*. 82, 1127-1132.

Srinivasula, S. M., Ahmad, M., Fernandes-Alnemri, T. & Alnemri, E. S. (1998) *Mol. Cell* 1, 949–957.

Stankiewicz, A., Lachapelle, G., Foo, CP., Radicioni, SM., Mosser, DD. (2005). *J Biol Chem* 280, 38729-38739.

Steel, R., Doherty, JP., Buzzard, K., Clemons, N., Hawkins, CJ., Anderson, RL. (2004). *J Biol Chem* 279, 51490-51499.

Stennicke, HR., Salvesen, GS. (2000). *Biochim Biophys Acta*. 1477, 299-306.

Susin, SA., Lorenzo, HK., Zamzami, N., Marzo, I., Snow, BE., Brothers, GM., Mangion, J., Jacotot, E., Costantini, P., Loeffler, M. et al. (1999). *Nature*. 397, 441-446.

Suzuki, Y., Imai, Y., Nakayama, H., Takahashi, K., Takio, K., Takahashi, R. (2001). *Mol Cell.* 8, 613-21.

Thompson CB. (1995). *Science.* 267, 1456-62.

Thornberry, N. A., Bull, H. G., Calaycay, J. R., Chapman, K. T., Howard, A. D., Kostura, M. J., Miller, D. K., Molineaux, S. M., Weidner, J. R., Aunins, J., et al. (1992) *Nature* 356, 768–774.

Thornberry, N. A., Lazebnik, Y. (1998) *Science* 281, 1312–1316.

Thornberry, N., Lazebnik, Y. (1998). *Science* 281, 1312-1316.

Vaesen, M., Barnikol-Watanabe, S., Gotz, H., Awni, LA., Cole, T., Zimmermann, B., Kratzin, HD., Hilschmann, N. (1994). *Biol Chem Hoppe Seyler.* 375, 113-26.

Van Loo, G., Van Gurp, M., Depuydt, B., et al. (2002). *Cell Death Differ.* 9, 20-26.

Vaux, DL., Silke, J. (2003). *Biochem Biophys Res Commun.* 304, 499-504.

Verhagen, AM., Ekert, PG., Pakusch, M., Silke, J., Connolly, LM., Reid, GE., Moritz, RL., Simpson, RJ., Vaux, DL. (2000). *Cell.* 102, 43-53.

Verhagen, AM., Silke, J., Ekert, PG., Pakusch, M., Kaufmann, H., Connolly, LM., Day, CL., Tikoo, A., Burke, R., Wrobel, C., Moritz, RL., Simpson, RJ., Vaux, DL. (2001). *J Cell Biol.* 152, 483-490.

Wang, CY., Mayo MW., Baldwin, Jr AS. (1996). *Science* 274, 784-787.

- Wang, X. (2001). *Genes Dev.* *15*, 2922-2933.
- Wellmann, A., Krenacs, L., Fest, T., Scherf, U., Pastan, I., Raffeld, M., Brinkmann, U. (1997). *Am J Pathol* *150*
- Willis, SN. and Adams, JM. (2005). *Curr Opin Cell Biol.* *17*, 617-625.
- Wu, G., Chi, J., Suber, TL., et al. (2000). *Nature* *408*, 1008-1012.
- Wu, CG., Hoek, FJ., Groenink, M., Reitsma, PH., van, Deventer SJ., Chamuleau, RA. (1997). *Int J Cancer.* *71*, 686-690.
- Wyllie, A. (1980a). *Nature* *284*, 555–556.
- Wyllie, A. H. (1980) *Nature* *284*, 555–556.
- Wyllie, A. H., Morris, R. G., Smith, A. L. & Dunlop, D. (1984) *J. Pathol.* *142*, 66–77.
- Wyllie, A., Kerr, JF., Currie, AR. (1980). *Int Rev Cytol.* *68*, 251-306.
- Wyllie, A., Kerr, JF., Currie, AR. (1980b). *Int Rev Cytol* *68*, 251-306.
- Yoshida, H., Kong, YY., Yoshida, R., Elia, AJ., Hakem, A., Hakem, R., Penninger, JM., Mak, TW. (1998). *Cell.* *94*, 739-750.
- Yu, X., Acehan, D., Menetret, JF., Booth, CR., Dudtke, ST., Riedl, SJ., Shi, Y., Wang, X., Akey, CW. (2005) *Structure* *13*, 1725-1735.
- Yuan, J., Shaham, S., Ledoux, S., Ellis, H. M. & Horvitz, H. R. (1993) *Cell* *75*, 641–652.

- Yuan, J.-Y., Horvitz, R. H. (1992) *Development* (Cambridge, U.K.) *116*, 309–320.
- Zhong, Q., Gao, W., Du, F., Wang, X. (2005). *Cell* *121*, 1085-1095.
- Zhou, L., Song, Z., Tittel, J. & Steller, H. (1999) *Mol. Cell* *4*, 745–755.
- Zhu, L., Perlaky, L., Henning, D., Valdez, BC. (1997). *Biochem Mol Biol Int.* *42*, 927-35.
- Zou, H., Henzel, WJ., Liu, X., Lutschg, A., Wang, X. (1997). *Cell* *90*, 405-413.
- Zou, H., Li, Y., Liu, X. & Wang, X. (1999) *J. Biol. Chem.* *274*, 11549–11556.

VITAE

Hyun-Eui Kim was born in Seoul, Korea, on September 3, 1974, the daughter of Young-Kyoo Kim and Eunsook Hwang. After completing her work and Saehwa girls' High School, Seoul, Korea in 1993, she entered Yonsei University in Seoul, Korea. She received the degree of Bachelor of Science with a major in biology from Yonsei University in March, 1997. She continued studying biology in the Graduate School of Science in Yonsei University and received the degree of Master of Science with a major in biology in March, 1999. In August, 2000 she entered the Graduate School of Basic Sciences at University of Texas Southwestern Medical School at Dallas. She did her graduate work with Xiaodong Wang, Ph.D. She plans to have her dissertation seminar in August, 2006.

Permanent address: Hanshin 16th Apt. 120-1005, Chamwon, Seocho,
Seoul, 137-030, Korea